JNeurosci
THE JOURNAL OF NEUROSCIENCE

Research Articles | Behavioral/Cognitive

Aperiodic EEG activity is a domain-specific marker of attentional aging in neurotypical adults

https://doi.org/10.1523/JNEUROSCI.1306-26.2026

Received: 29 July 2026
Revised: 25 September 2026
Accepted: 17 October 2026

Copyright © 2026 the authors

This Early Release article has been peer reviewed and accepted, but has not been through the composition and copyediting processes.The final version may differ slightly in style or formatting and will contain links to any extended data.

Alerts: Sign up at www.jneurosci.org/alerts to receive customized email alerts when the fully formatted version of this article is published.

Title

Aperiodic EEG activity is a domain-specific marker of attentional aging in neurotypical adults

Abbreviated Title

Aperiodic Exponent Tracks Attentional Aging

Names and Affiliations

Christian Cazares[1], Alison Rigby[2], Leena Kang[1], Stephan Getzmann[3], Stefan Arnau[3], Edmund Wascher[3,4], Bradley Voytek[1,2,5,6]

1 Department of Cognitive Science, University of California, San Diego, La Jolla, California, 92037

2 Neurosciences Graduate Program, University of California, San Diego School of Medicine, La Jolla, California, 92037

3 Leibniz Research Centre for Working Environment and Human Factors (IfADo), Dortmund, 44139, Germany

4 German Center for Mental Health (DZPG), Partner Site Bochum-Marburg, Bochum, 44787, Germany

5 Halıcıoğlu Data Science Institute, University of California, San Diego, La Jolla, California, 92037, USA

6 Kavli Institute for Brain and Mind, University of California, San Diego, La Jolla, California, 92037, USA

Corresponding Author: Christian Cazares, cacazares@ucsd.edu

JNeurosci Accepted Manuscript

Number of Pages: 47

Number of Figures: 6

Number of Tables: 1

Number of Multimedia: 0

Number of 3D Models: 0

Conflicts of Interest

The authors declare no competing financial interests.

Acknowledgements

We'd like to thank Dr. Dillan Cellier and Dr. Maribel Patiño for their thoughtful feedback and discussion. C.C. was supported by a NIH/NIMH Blueprint D-SPAN Award (K00 MH132569), a NIH/NIGMS IRACDA Award (K12 GM068524), and the Burroughs Wellcome Fund.

JNeurosci Accepted Manuscript

Abstract

Aperiodic neural activity has been reliably shown to be reduced among older adults, and these reductions are associated with age-related cognitive decline. These results suggest that aperiodic activity, as measured by the spectral exponent, might be a viable electrophysiological biomarker for cognitive aging. However, this has not been tested longitudinally, within participants, during normal aging. Here, we used a longitudinal cohort of either sex to test whether changes in aperiodic activity between two sessions, approximately 5 years apart, track behavioral change across two domains: sustained attention (Psychomotor Vigilance Test) and executive function (modified Simon task). We found that aperiodic activity declined within individuals after the interval, independent of age at baseline. This within-person change tracked concurrent changes in reaction times during sustained attention but was not associated with changes in any Simon task measure. Within a resampling framework, the aperiodic-PVT association was stable across cohort resamples and independently fitted partitions, though it was not confirmed in a small, frozen held-out set. These findings suggest the longitudinal decline in aperiodic activity tracks attentional processing speed rather than executive function, supporting its potential as a domain-specific biomarker of attentional aging in neurotypical populations.

Significance Statement

Aperiodic (non-oscillatory) neural activity, indexed by the aperiodic exponent, is known to decline in older adults, but whether this happens within individuals over just a few years, and in step with cognitive change, remains unclear. Here we leveraged scalp EEG and cognitive-behavioral data from 276 neurotypical adults, tested twice approximately five years apart, and found that the aperiodic exponent declines within individuals over this interval, independent of

JNeurosci Accepted Manuscript

age at baseline. This decline tracked concurrent slowing on a sustained attention task, but not change on an executive function task, and only in EEG recorded before, not after, cognitive testing. Based on this dissociation, we propose that aperiodic exponent decline indexes attentional processing speed rather than general cognitive decline in neurotypical aging.

Introduction

The U.S. population aged 65 and older is growing faster than any other age group (Roberts, A. W. et al., 2018) and is at the highest risk for age-related cognitive decline (Baddeley et al., 1991, 2001; Agüero-Torres et al., 2002; Hugo and Ganguli, 2014), creating an urgent need for objective, scalable neural markers of within-person cognitive change. Aging compromises sustained attention (Fortenbaugh et al., 2015), information-processing speed (Vallesi et al., 2021), and executive function (Erb et al., 2023), but how to index the underlying neural processes non-invasively remains unclear.

Oscillatory and evoked scalp electroencephalography (EEG) measures, including peak alpha frequency, alpha-band power and connectivity, and P300 latency and amplitude, covary with age and cognition (Fjell et al., 2007; van Dinteren et al., 2014; Lejko et al., 2020; Cesnaite et al., 2023; Merkin et al., 2023; Park et al., 2024). However, some of these effects are partly non-oscillatory (Merkin et al., 2023). Thus, an emerging alternative to tracking age effects is the aperiodic (broadband, non-oscillatory) component (Miller, 2010; Buzsáki et al., 2012; He, 2014; Voytek et al., 2015; Donoghue et al., 2020), indexed by the aperiodic exponent (the log-log slope of the 1/f-like spectrum), which is physiologically distinct from narrowband oscillations (Donoghue et al., 2020, 2022). Mechanistically, the exponent has been linked to cortical excitation/inhibition (E/I) balance (Gao et al., 2017; Wiest et al., 2023; Wang et al., 2026), though many other factors likely contribute (Marinazzo, 2026; Preston et al., 2026). In

JNeurosci Accepted Manuscript

neurotypical and compromised aging the exponent decreases (the spectral slope “flattens”), indexing a shift toward excess excitation with loss of inhibition (Voytek and Knight, 2015; Voytek et al., 2015; Dave et al., 2018; Gao et al., 2020; Tran et al., 2020; Finley et al., 2024; Wilkinson et al., 2024; Ranasinghe et al., 2025; Politanskaia et al., 2026). Work across neural scales supports this interpretation but shows it depends on methodology and cell type (Chini et al., 2022; Avila et al., 2024; Brake et al., 2024; Campbell et al., 2024; Salvatore et al., 2024; Chakravarty et al., 2025; Pré et al., 2026; Sheldon et al., 2026).

Cross-sectional studies consistently show a lower exponent in older adults (Voytek et al., 2015; Merkin et al., 2023; Avila et al., 2024) and has been linked to attention and memory (Lendner et al., 2020; Cunningham et al., 2023; Merkin et al., 2023; Montemurro et al., 2024; McKeown et al., 2025; Wang et al., 2026). Longitudinal studies have instead mostly covered childhood through mid-adolescence (McSweeney et al., 2021; Wilkinson et al., 2024; Antúnez et al., 2025), or stroke recovery in adults (Lanzone et al., 2022). One study confirmed that the exponent decreases over multiple years in adults aged 20 to 70 (Politanskaia et al., 2026), consistent with findings over up to one year (Li et al., 2024; Uudeberg et al., 2025). Whether within-person exponent change tracks cognitive-behavioral change remains unknown, as is whether any coupling is general, consistent with a broad neural noise account, or domain-specific, as seen when aperiodic measures track decline in episodic and visual short-term but not working memory (McKeown et al., 2025; Campbell et al., 2026).

Here we analyzed neurotypical adults from the Dortmund Vital Study (Gajewski et al., 2022; Getzmann et al., 2024) with task-free EEG recorded before and after cognitive-behavioral assessments at two timepoints approximately five years apart. To dissociate domain-general from domain-specific effects, we used the Psychomotor Vigilance Test (PVT), indexing sustained attention and processing speed (Dinges and Powell, 1985; Wascher et al., 2022), and

JNeurosci Accepted Manuscript

a modified Simon task, indexing executive function and interference control (Simon, 1969; Hoppe et al., 2017). The exponent declined within individuals (as in Politanskaia et al., 2026), independent of baseline age, alongside PVT slowing. Exponent change tracked PVT slowing, but no Simon measure, after controlling for baseline age, exponent, performance and sex, and only when EEG preceded the assessments, suggesting that longitudinal aperiodic decline tracks attentional rather than general cognitive aging.

Methods

Participants and study design

We analyzed data from a finalized count of 276 neurotypical adults from the Dortmund Vital Study (Gajewski et al., 2022; Getzmann et al., 2024), an ongoing longitudinal cohort study of cognitive aging across adults aged 20 to 70 years conducted at the Leibniz Research Centre for Working Environment and Human Factors at the Technical University of Dortmund, Germany (IfADo; ClinicalTrials.gov NCT05155397). Each analyzed participant had complete task-free EEG and cognitive-behavioral assessments at two timepoints approximately five years apart (5.3 ± 0.8 years; mean ± SD). Participants were recruited from local companies and public institutions and through public advertisements. Exclusion criteria comprised a history of severe disease, namely neurological disease (such as dementia, Parkinson's disease or stroke), cardiovascular, oncological and eye disease, psychiatric and affective disorders, head injury, head surgery or head implants, the use of psychotropic drugs and neuroleptics, and limited physical fitness or mobility. Common medications such as blood thinners, hormones, antihypertensives and cholesterol-lowering agents were not grounds for exclusion. Participants reported being healthy and free of medication that could affect attention during the experimental

JNeurosci Accepted Manuscript

sessions. All participants gave written informed consent and the study conformed to the Declaration of Helsinki with approval by the local Ethics Committee of the Leibniz Research Centre for Working Environment and Human Factors, Dortmund (approval A93-1, and A93-3 for the follow-up). The present sample additionally draws on follow-up data beyond the original release (see Data availability). Participant's age at second session was not exact, but rather reconstructed from the recording years in the BIDS session files as the baseline age plus the elapsed interval.

Cognitive-behavioral assessments

At each session participants completed a standardized cognitive test battery (Gajewski et al., 2022). The present analyses used two of these tasks, selected for the minimal contrast required to test domain specificity: Sustained attention and processing speed were measured with a ten-minute psychomotor vigilance task (PVT)(Dinges and Powell, 1985; Wascher et al., 2022) adapted to present the target ("+") at one of four random interstimulus intervals (2, 3, 5 or 8 s), with the screen blank during the interval. Participants responded to each target onset with a button press as quickly as possible. We computed mean reaction time, reaction-time variability and the proportion of correct responses, each averaged across the five consecutive two-minute blocks of the ten-minute task. Executive function, interference control, and response inhibition were measured with a modified version of the Simon task comprising intermixed 'Go' and 'No-Go' trials (Simon, 1969; Hoppe et al., 2017). On each trial a target appeared to the left or right of fixation, and participants responded with a left- or right-hand keypress according to the non-spatial target feature (letter "H" or "N") while the task-irrelevant target location varied independently. 'No-Go' trials, signaled by a surrounding diamond, required the response to be withheld. Among 'Go' trials, signaled by a surrounding circle, we distinguished congruent trials (target location and response side on the same side) from incongruent trials (opposite sides)

JNeurosci Accepted Manuscript

and defined the Simon effect as the difference in mean response time between incongruent and congruent 'Go' trials. We used mean 'Go' response time across all 'Go' trials, and 'No-Go' accuracy (the proportion of 'No-Go' trials on which the response was correctly withheld) as an index of response inhibition. Measures from the remaining assessments in the Dortmund Vital Study battery were not part of the data use agreement used in this study.

EEG data acquisition

Task-free scalp EEG was recorded with a 64-channel elastic cap, electrodes connected with saline solution and arranged according to the international 10-20 system, using a BrainVision BrainAmp DC amplifier and BrainVision Recorder software (Brain Products GmbH) with channel 'FCz' as the online reference. Signals were digitized at 1000 Hz with a 250-Hz online low-pass filter and no online high-pass filter, and electrode impedances were kept below 10 kOhm. At each session, task-free EEG was acquired for three minutes with eyes closed and three minutes with eyes open, always in that order, and this pair of recordings was obtained both before (pre) and after (post) the approximately two-hour cognitive-behavioral task battery, yielding four resting recordings per session roughly two hours apart. All testing was conducted in the morning at a fixed time across participants to standardize wakefulness.

EEG preprocessing

Preprocessing was performed in MNE-Python (Gramfort et al., 2014) (see the Software section for all package versions used in our analyses). Continuous recordings were assigned the 64-channel 10-20 montage. Line noise was attenuated with a spectrum-fit notch filter at 50 Hz and its first harmonic (100 Hz), and the data were band-pass filtered between 1 and 100 Hz with a zero-phase FIR filter (Hamming window) before re-referencing from the 'FCz' online reference

JNeurosci Accepted Manuscript

to the common average. Ocular, muscular and other non-neural artifacts were removed with independent component analysis ('extended Infomax', 20 components), with the decomposition fitted under a peak-to-peak amplitude 'global' rejection threshold estimated by AutoReject (Jas et al., 2017) so that high-amplitude segments did not dominate the solution. Components were classified with ICLabel (Pion-Tonachini et al., 2019) as implemented in mne-icalabel (Li et al., 2022), which returns a probability for each of seven component classes (brain, muscle, eye, heart, line noise, channel noise, other). Each component was assigned to its highest-probability class, with no minimum probability required, and all components not assigned to 'brain' or 'other' were discarded before back-projection. Across the 2,206 task-free recordings from the 276 analyzed participants (two post-task recordings were unavailable), a mean of 8.42 of 20 components were excluded per recording (SD 3.78, median 8, range 0 to 18), comprising predominantly muscle (mean 5.61 per recording) and ocular (mean 2.12) components. The post-processed data were segmented into non-overlapping ten-second epochs, and residual bad epochs were rejected or repaired with AutoReject (via calculation of local high-amplitude rejection thresholds). Finally, a 100-ms Hamming taper was applied to the leading and trailing edges of each epoch to limit spectral leakage that may occur when non-consecutive post-processed epochs were appended.

Spectral parameterization

Power spectral densities were estimated from the artifact-corrected epochs using Welch's method (one-second Hamming window, 50% overlap, two-second zero-padded FFT length, median across windows) over 1 to 80 Hz, and the resulting per-epoch spectra were combined across epochs by their median to give a single spectrum per channel that was then parameterized with the *specparam* algorithm (formerly FOOOF) (Donoghue et al., 2020), fitted over 1 to 45 Hz in the primary analysis, with peak width limits of 2 to 12 Hz, no limit on the

JNeurosci Accepted Manuscript

number of peaks, a minimum peak height of 0 and a peak threshold of 2 standard deviations. The one-second window was selected to match prior EEG work applying *specparam* (Smith et al., 2023) and yields a median of 340 segments per channel across the recording. This window resolves only one cycle at 1 Hz, so the lowest frequencies in the fitting range are estimated with less precision. For every channel we fitted two aperiodic models, one assuming a single power law ('fixed' mode) and one incorporating a spectral knee ('knee' mode). To confirm that the choice of fit range did not drive results, the full pipeline was repeated with upper fit bounds of 35 and 40 Hz as a sensitivity analysis. Because of the resolution limit noted above, we also repeated it with a lower fit bound of 3 Hz, which excludes the frequencies resolved by fewer than three cycles, holding the aperiodic mode selection at the 1 to 45 Hz decision so that only the lower bound differed. While the aperiodic exponent was the primary feature of interest, we additionally computed the aperiodic-adjusted peak power within delta (1 to 4 Hz), theta (4 to 7 Hz), alpha (7 to 13 Hz) and beta (13 to 24 Hz) bands, specifically the height of the largest spectral peak above the aperiodic fit within each band.

Because a spectral 'knee' may or may not be visually present in each power spectra, we selected the *specparam* aperiodic mode per participant and per task rather than imposing this mode on the whole sample. Therefore, for each participant by eye-condition combination we compared the model outputs from individually fitted 'fixed' and 'knee' modes using the adjusted R^2 of the fit over a low-frequency subrange (1 to 20 Hz), averaged across that participant's baseline recordings. The 'knee' model was adopted only when it improved adjusted R^2 over the 'fixed' model and its estimated 'knee' frequency fell within the fitted range, suggesting the presence of a biophysically plausible 'knee', otherwise the 'fixed' model was retained. The selected mode was then applied to all participant by eye-condition combination recordings across both sessions, and these mode-validated outputs, such as the aperiodic exponent, were used in all primary analyses.

JNeurosci Accepted Manuscript

Model fits were also subjected to a channel-level quality gate before any averaging: channels whose fit explained less than 90% of the spectral variance (R^2 below 0.9) were removed from the average. Summaries were formed for five scalp EEG electrode regions (frontal: ‘Fp1’, ‘Fp2’, ‘F3’, ‘AF3’, ‘F5’, ‘F1’, ‘FC3’, ‘F4’, ‘AF4’, ‘F6’, ‘F2’, ‘FC4’, ‘Fz’; temporal: ‘T7’, ‘FT7’, ‘TP7’, ‘T8’, ‘FT8’, ‘TP8’; central: ‘C3’, ‘C5’, ‘C1’, ‘CP3’, ‘C4’, ‘C2’, ‘C6’, ‘CP4’, ‘Cz’; parietal: ‘P3’, ‘P5’, ‘P1’, ‘P7’, ‘Pz’, ‘P4’, ‘P6’, ‘P2’, ‘P8’; occipital: ‘O1’, ‘O2’, ‘Oz’, ‘PO7’, ‘PO3’, ‘POz’, ‘PO4’, ‘PO8’), each requiring at least two surviving channels to be computed, and together with the whole-scalp average these constituted the six electrode groupings used in the regional robustness analyses. A participant was flagged for exclusion if fewer than 32 channels survived the gate in each recording (n=17 participants, not included in the final count). Unless otherwise stated, analyses used the whole-scalp average exponent across surviving channels for a total of 276 participants. Across pre-task recordings, model R^2 was 0.973 eyes-open and 0.984 eyes-closed, 95.3% versus 98.8% of channels met the $R^2 \geq 0.90$ criterion, and mean absolute fitting error was 0.040 versus 0.047.

Statistical analyses

Overview of the analyses. All analyses were performed using the training set (n = 222) unless stated otherwise, and on pre-task recordings unless an acquisition contrast is reported. We first established that the aperiodic exponent and each behavioral measure changed between baseline and follow-up, correcting within each outcome domain: the aperiodic exponent under two recording conditions (m = 2), the three PVT measures (m = 3), and the three Simon measures (m = 3). We then tested the between-person age gradient of the same eight measures under the same three families. The primary brain-behavior analysis asked whether within-person exponent change was associated with concurrent behavioral change, reported for

JNeurosci Accepted Manuscript

the whole-scalp average of eyes-open recordings fitted over 1 to 45 Hz and corrected across the full grid of six electrode groupings, three task measures, two recording conditions and three spectral fitting ranges (m = 108 per task), separately within the PVT and modified Simon task analyses. A companion model added the concurrent band-power changes and was corrected across its five Δ-spectral terms. As secondary analyses we tested whether the coupling differed by recording condition and by pre- versus post-task acquisition, correcting the two interaction contrasts together. Finally, we assessed the stability of the coupling under resampling and its generalization in the frozen held-out set (n = 54).

Held-out validation split. To provide an unbiased test of predictive generalization, we defined a single train/test split *a priori* and froze it for all downstream analyses. Participants with complete pre-task EEG recordings in both conditions at both sessions, complete behavioral data at both sessions, and no recording excluded by the R^2 gate were eligible. We allocated 20% of eligible participants to a held-out test set (n = 54) and the remaining 80% to a training set (n = 222), stratifying the allocation by baseline age band (under 30, 30 to 50, 50 to 70 and 70 or over years) so that the age distribution was preserved across sets. The split was generated once with a fixed random seed and stored as a fixed reference and no subsequent analysis altered it. The two sets were compared on baseline age with a Mann-Whitney U test and on sex with a chi-squared test and did not differ on either. All analyses, unless stated otherwise, used the training set (n = 222).

Longitudinal and cross-sectional effects. Aperiodic exponent and behavioral measures were tested to see whether they changed across the follow-up. Within-person changes were tested with two-sided paired t-tests and corroborated with sign-flip permutation tests (see Permutation tests). Effect sizes were reported as Cohen's d_z, with all differences signed as follow-up minus baseline. To confirm that any within-person change was not an artifact of baseline-dependent

JNeurosci Accepted Manuscript

change, we regressed each change score on its own baseline level and inspected the intercept at the mean baseline. The follow-up interval was included in the same models because participants differed in how much time elapsed between sessions. Longer intervals span more aging, so a positive coefficient on this term would indicate change accumulating with elapsed time rather than a nuisance to be removed. We then residualized the change on baseline level, sex and interval and tested its dependence on baseline age. To confirm that the exponent decline was not a by-product of concurrent oscillatory power changes, we regressed the within-person exponent change on the concurrent within-person changes in delta, theta, alpha and beta aperiodic-adjusted peak power, with baseline age and sex.

To separate the between-person age gradient from within-person change, we fitted linear mixed-effects models of each EEG and behavioral measure with a fixed effect of session, baseline age and sex and a by-participant random intercept (*measure ~ session + age + sex + (1 | participant)*). The session term estimated the within-person change across the follow-up and the age term estimated the cross-sectional gradient. Raw coefficients (β) are reported in natural units with 95% confidence intervals and exact p-values, unless stated otherwise.

Unless a contrast between acquisitions is explicitly reported, every analysis in this manuscript used pre-task recordings. This applies to the longitudinal change tests, the cross-sectional age models, and all coupling models, including the robustness grids across electrode groupings, spectral fitting ranges and recording conditions. Post-task recordings were fitted only for the acquisition-by-exponent interaction and within the predictive-modeling framework, where pre- and post-task models are compared on identical participants.

Brain-behavior coupling and state specificity. Our central analysis asked whether within-person change in EEG measures tracked concurrent change in each cognitive-behavioral

JNeurosci Accepted Manuscript

measure. Primary analyses used the eyes-open, pre-task recordings, which were acquired immediately before the task battery, are matched in eye state to the tasks, and are less susceptible to drowsiness. Eyes-closed recordings were retained as a designated comparison condition. Across the pooled baseline and follow-up sessions we first related the measure to the exponent with ordinary least squares using cluster-robust standard errors (clustered by participant), including an exponent-by-session interaction to test whether the cross-sessional relationship changed over time. The primary test then used within-person change scores, computed as follow-up minus baseline for every measure: we regressed cognitive change on exponent change, adjusting for baseline cognitive performance, baseline exponent, baseline age, sex and the per-person follow-up interval. Baseline age was mean centered within the analysis sample (n=222) rather than across the full cohort (n=276) until predictive analyses were performed. Coefficients are reported in their natural units, for example milliseconds of reaction-time change per unit change in the exponent, with 95% confidence intervals and exact p-values unless $p < 0.001$.

To test whether coupling was specific to the aperiodic exponent rather than to oscillatory features, we additionally regressed each cognitive-behavioral change on the concurrent change in the exponent together with the concurrent changes in delta, theta, alpha and beta aperiodic-adjusted peak power, the baseline level of each spectral term and the same covariates and controlled the false discovery rate across this five-term spectral family. For this model the concurrent band-power changes were each divided by their standard deviation (expressed in per-standard-deviation units) so that their coefficients would be comparable as effect sizes, while the outcome and the age and sex terms remained in raw units. All change-score and coupling models were refitted across the three spectral fitting ranges (1 to 35, 1 to 40 and 1 to 45 Hz), the six electrode groupings and both recording conditions for a sensitivity analysis.

JNeurosci Accepted Manuscript

To test whether coupling depended on recording condition or on pre- versus post-task acquisition, we fitted two interaction contrasts. Within-condition coupling was estimated with ordinary least squares on change scores, one row per participant. Because each participant contributes one behavioral change score but two exponent change scores, one per condition or acquisition, the between-condition and between-acquisition contrasts were fitted with one row per participant, regressing the behavioral change on the difference between the two exponent changes and on their mean, so that the coefficient on the difference term is the interaction. We used this form rather than a mixed model because the outcome does not vary within participant, which makes a by-participant random intercept degenerate. The two interaction contrasts were corrected together as a family.

Multiple-comparison correction and permutation tests. Where a family of related tests was performed, we controlled the false discovery rate ($q < 0.05$) with the Benjamini-Hochberg procedure (Benjamini and Hochberg, 1995). For the longitudinal change tests and the cross-sectional age terms, correction was applied within each outcome family: the aperiodic exponent under two recording conditions, the three PVT measures, and the three Simon measures. For the exponent and behavioral coupling models, the *Δexponent* term was corrected across the full coupling grid of 108 tests per task, spanning six electrode regions, three task measures, two recording conditions and three spectral fitting ranges, separately within the PVT and Simon analyses, whereas the joint spectral model was corrected across its five-term Δ-spectral family. The two interaction contrasts were corrected together as a family. Effects that pass the uncorrected but not the corrected threshold are described as non-significant.

We corroborated all within-person changes and coupling effects with non-parametric permutation tests. For each test the differences within-person were randomly multiplied by plus or minus one across 10,000 permutations and the one-sample t-statistic was recomputed. The

Neurosci Accepted Manuscript

two-sided p-value was thus the proportion of permuted statistics whose magnitude met or exceeded the initial observation, with the smallest reportable value being $p < 1 \times 10^{-4}$.

Predictive modeling and held-out validation. To test whether the within-person exponent decline that tracked PVT slowing reflected a stable, behaviorally specific signal rather than a single-sample association, we refitted the model across 200 age-stratified 80/20 resamples of the training set (n = 222). This framework was fitted to eyes-open recordings, with pre-task and post-task acquisitions fitted separately for comparisons. Two training participants were each missing a post-task eyes-open recording at one of the two sessions, so all post-task models, and the paired pre-versus-post comparisons that require both recordings from the same participant, were fitted to the 220 participants with complete pre- and post-task data. The held-out test set was complete for both recordings (n = 54). Each resample fitted the model on an 80% partition and evaluated it on the held-out 20%, so these repeated within-training splits index the stability of the coupling rather than independent generalization, for which we reserved the *a priori* held-out set (n = 54).

Every model in this framework used the brain-behavior coupling predictor set, namely the change in the exponent and its interaction with baseline age, the baseline exponent, baseline reaction time, baseline age, sex and the per-person follow-up interval, so that the resampled coefficient would be directly comparable with the primary coupling estimate. Within each resample the coupling coefficient was estimated separately in the training and held-out partitions, and we reported their sign concordance. To isolate the contribution of the exponent from the shared, baseline-driven prediction that arises through regression to the mean, we computed the paired difference in held-out R^2 between the pre-task and post-task models on identical participants (the pre-minus-post increment) and tested it against a two-sided full label-shuffle null (1,000 permutations across 100 folds), the statistic being the mean ΔR^2 across the

JNeurosci Accepted Manuscript

100 folds. To compare feature use across cognitive-behavioral domains on a common scale, we fitted a penalized (ElasticNet) model whose penalty was tuned by five-fold cross-validation on the training data (the L1 ratio searched over 0.1 to 1.0), with predictors standardized within each fold, and expressed the exponent weight after dividing by the within-fold outcome standard deviation, recording how often the weight survived the L1 penalty across resamples. The penalty was tuned independently within each arm, so the selected penalties differ across models (Table S2). We therefore report the standardized weights, which do not depend on the penalty, alongside the selection rates. As a confirmatory test on the *a priori* held-out set (n = 54), we refit the coupling model within the held-out set to obtain its coupling coefficient and separately applied the frozen training model to predict held-out reaction-time change to obtain an out-of-sample R^2, both of which we report together with the percentile at which they fell in the training-resample distribution.

Software

All preprocessing, spectral parameterization, statistical analysis and visualization were carried out in Python (3.9.19), using MNE-Python (Gramfort et al., 2014) (1.8.0) for EEG handling and preprocessing, mne-icalabel (Li et al., 2022) (0.7.0) for ICLabel (Pion-Tonachini et al., 2019) component classification, AutoReject (Jas et al., 2017) (0.4.3) for epoch rejection and threshold estimation, *specparam* (Donoghue et al., 2020) (2.0.0rc6) for spectral parameterization, statsmodels (Skipper and Perktold, 2010) (0.14.4) for the regression and mixed-effects models, scikit-learn (1.4.2) for the ElasticNet models, h5py (3.11.0) for reading the behavioral data, and NumPy (Harris et al., 2020) (1.26.4), pandas (1.5.3), SciPy (1.13.1), Matplotlib (Hunter 2007) (3.9.0) and seaborn(Waskom, 2021) (0.13.2) for numerical work and plotting.

Data availability

JNeurosci Accepted Manuscript

A subset of the EEG data analyzed in this study (n=208 participants, baseline release) is available at OpenNeuro (dataset accession number: ds005385, 10.18112/openneuro.ds005385.v1.0.2). The most up-to-date raw EEG and behavioral data (including the n = 276 used in this study after processing) is available upon reasonable request to Drs. Getzmann and Wascher. The present analyses were performed under a data use agreement that covered the longitudinal EEG, demographic variables, and behavioral results from the psychomotor vigilance and modified Simon tasks. Other assessments in the Dortmund Vital study battery require separate arrangements with the study investigators.

Code availability

All code used to recreate figures is publicly available on GitHub: https://github.com/voytekresearch/Adult_EEG_Dortmund.

Results

The aperiodic exponent declines in neurotypical adults

We analyzed a dataset from 276 neurotypical adults with task-free EEG measured before and after a 2-hour block of cognitive-behavioral testing across two timepoints that were an average of 5 years apart (5.3 ± 0.8 years, mean ± SD; 166 females). At both timepoints, three minutes of EEG was collected under two conditions, eyes closed and eyes open, before (pre-task) and after (post-task) completing the PVT and Simon tasks (**Fig. 1A**). Data from the full cohort was split *a priori* into a training set (n = 222; 131 females) and a held-out test set (n = 54; 35 females) reserved for the later predictive analyses, stratified to match in baseline age (Mann-

JNeurosci Accepted Manuscript

Whitney U = 5,864, p = 0.80) and sex ($\chi^2(1) = 0.39$, p = 0.53) (**Fig. 1B**) (**Table 1**). All remaining analyses used the training set until predictive analyses were performed.

Across baseline and follow-up sessions, task-free EEG power spectra followed the canonical aperiodic (1/f-like) relationship (**Fig. 1C**). The aperiodic component fitted to the participant-averaged spectra for all electrodes was 'flatter' at follow-up, consistent with a reduced aperiodic exponent. The exponent declined in both task-free conditions (eyes open mean change = -0.040, 95% CI [-0.059, -0.020], permutation sign-flip test corrected $p = 1 \times 10^{-4}$, $d_z = -0.26$; eyes closed mean change = -0.045, 95% CI [-0.066, -0.024], corrected $p < 1 \times 10^{-4}$, $d_z = -0.28$) (**Fig. 1D**). This decline was also present when the spectral parameterization lower bound was raised from 1 to 3 Hz (eyes open mean change = -0.031, 95% CI [-0.055, -0.006], versus -0.043 in the same participants at 1 to 45 Hz; n = 219, since three participants fell below the channel-quality criterion at baseline over the shorter range). This decline did not differ between eyes-open and eyes-closed conditions (sign-flip permutation test, paired t(221) = 0.46, p = 0.64, $d_z = 0.03$). Primary analyses used the eyes-open, pre-task recordings because these recordings were acquired immediately before the task battery, are matched in eye state to the tasks themselves, and are less susceptible to drowsiness. Eyes-closed recordings were retained as a designated comparison condition for the state-specificity analyses reported below. Visually, this aperiodic exponent decline was spatially distributed across the scalp (mean change = -0.04) (**Fig. 1E**).

To separate cross-sectional age differences from longitudinal change, we fitted a linear mixed-effects model of the exponent. Older ages at baseline were associated with a lower aperiodic exponent between individuals (β = -0.0053 per year, 95% CI [-0.0071, -0.0035], corrected p < 0.001), and independently of this gradient, the aperiodic exponent declined within individuals (β = -0.040, 95% CI [-0.059, -0.020], corrected p < 0.001), with no sex effect (β = +0.026, 95% CI [-0.023, 0.076], uncorrected p = 0.29) (**Fig. 1F, G**) (see **Table S1**). To test if the exponent decline

JNeurosci Accepted Manuscript

was driven by concurrent shifts in oscillatory power, we regressed the within-person exponent change on the concurrent within-person changes in delta (1 to 4 Hz), theta (4 to 7 Hz), alpha (7 to 13 Hz), and beta (13 to 24 Hz) band aperiodic adjusted power, together with age at baseline and sex. No band-power change predicted the observed exponent changes (all FDR-corrected $p > 0.05$) (**Fig. 1H**), indicating that the decline was not merely a by-product of changes in oscillatory-power. To confirm that the mean exponent decline was robust to spectral parameterization fitting ranges, we refitted the within-person model across three spectral fitting ranges (1 to 35, 1 to 40, 1 to 45 Hz) and six regional electrode groups (**Fig. 1I**). The cross-session change coefficient was negative in all 18 cells and survived correction across this grid in 17 of them, the exception being the central region at 1 to 45 Hz ($\beta = -0.009$, corrected $p = 0.376$), suggesting that the within-person aperiodic decline was a stable neural measure for the behavioral analyses that followed.

Attentional reaction time slows in neurotypical adults

We next characterized the aging-related change in sustained attention and processing speed as assayed by the PVT (**Fig. 2A**). In a linear mixed-effects model, mean reaction time rose across the ten-minute task and this time-on-task increase did not differ between sessions (*bin*, $\beta = 7.9$ ms per 2-min bin, 95% CI [6.48, 9.42], $p < 0.001$; *bin x session*, $\beta = 0.80$, 95% CI [-1.27, 2.88], $p = 0.45$) (**Fig. 2B**). Mean reaction time increased from baseline to follow-up (mean change = 10.5 ms, 95% CI [3.076, 17.979]; sign-flip permutation test, paired $t(221) = 2.76$, raw $p = 0.007$, corrected $p = 0.020$, $d_z = 0.19$) (**Fig. 2C**), whereas neither reaction time variability nor response accuracy changed over the same interval (sign-flip permutation test raw $p = 0.448$ and 0.381, corrected $p = 0.448$ for both) (**Fig. S1A, B**). Linear mixed-effects models of each measure (*measure ~ session + age + sex + (1 | participant)*) confirmed these within-person changes and separated them from the between-person age gradient. Cross-sectionally, older baseline age

JNeurosci Accepted Manuscript

was associated with faster baseline reaction time, opposite to the within-person slowing (β = -0.529 ms per year, 95% CI [-1.02, -0.04], raw p = 0.034), although this gradient did not survive correction across the three PVT measures (corrected p = 0.102) (**Fig. 2D, E**) (see **Table S1**).

Because change scores are subject to regression to the mean, we modeled the change in mean reaction time directly, adjusting for baseline mean reaction time and baseline age, and including the follow-up interval since participants followed for longer have had more time to change. Baseline mRT predicted the change (β = -0.44 ms per ms baseline RT, 95% CI [-0.57, -0.32], p < 0.001, adj. R^2 = 0.17), with slower participants at baseline tending to become faster (**Fig. S1C**). The mean increase nonetheless survived this adjustment (intercept at mean baseline = 10.5 ms, 95% CI [3.70, 17.36], p < 0.001). After residualizing the change on baseline performance and follow-up interval, neither baseline age (β = -0.23 ms per year, 95% CI [-0.75, 0.30], p = 0.40) nor follow-up interval (β = 3.73 ms per year, 95% CI [-5.34, 12.79], p = 0.42) predicted its magnitude (**Fig. S1D**), suggesting a cohort-wide, within-person slowing rather than an effect concentrated in older participants or moderated by any specific time-interval between sessions.

The aperiodic exponent tracks concurrent attentional reaction time slowing.

We next investigated whether the aperiodic exponent was correlated with the observed PVT mean reaction time increase. Across the pooled baseline and follow-up sessions, mean reaction time did not correlate with the exponent (β = 15 ms per unit, 95% CI [-24.52, 54.52], uncorrected p = 0.46, baseline r = 0.1, follow-up r = -0.04), although the slope relating the exponent to reaction time was marginally more negative at follow-up (*exponent x session*, β = -41.5 ms, 95% CI [-82.95, -0.09], uncorrected p = 0.049) (**Fig. 3A**). Within individuals, participants with a greater decline in the exponent showed a greater increase in mean reaction time (r(220) = -

JNeurosci Accepted Manuscript

0.17, p = 0.010) (**Fig. 3B**), and this relationship was driven by the exponent change rather than the baseline exponent (r(220) = 0.027, p = 0.69) (**Fig. 3C**). Both bivariate relationships remained when assessed using a multivariable model that included the change and the baseline exponent simultaneously, together with baseline age, baseline reaction time, sex and the follow-up interval. In this model, each one-unit decrease in the exponent corresponded to a 91 ms increase in reaction time (*Δexponent*, β = -91.11 ms, 95% CI [-142.63, -39.59], raw p < 0.001, FDR-corrected p = 0.027 across the 108-test coupling grid), whereas the baseline exponent remained non-significant (β = -11.9 ms, 95% CI [-49.37, 25.48], p = 0.53; adjusted R^2 = 0.21) (**Fig. 3D**). This coupling was also present when the spectral parameterization lower bound was raised from 1 to 3 Hz (β = -46.80, 95% CI [-88.12, -5.49], p = 0.027, n = 219; three participants fell below the channel-quality criterion at baseline over the shorter range). This relationship was not moderated by baseline age (*Δexponent x baseline age*, β = -0.81, 95% CI [-4.02, 2.40], p = 0.62), suggesting a cohort-wide, within-person effect. The follow-up interval was included as a covariate since participants followed for longer have had more time to change. Its coefficient was positive, in the direction an accumulating effect would predict, but not significant (β = 4.1 ms per year, 95% CI [-4.80, 12.99], p = 0.37). Baseline reaction time was negatively related to its own change (β = -0.47, 95% CI [-0.59, -0.34], p < 0.001) consistent with regression to the mean, but the exponent coupling held over and above this dependence.

To test whether this effect was specific to the aperiodic exponent rather than to oscillatory features, we regressed the within-person change in mean reaction time on the concurrent change in the exponent and in delta, theta, alpha and beta band aperiodic-adjusted power, together with the baseline level of each spectral term, baseline age, baseline reaction time, sex and the follow-up interval. Of the five simultaneous spectral-change terms, only the exponent change predicted reaction time change after correction (β = -85.9 ms, 95% CI [-137.38, -34.45],

JNeurosci Accepted Manuscript

FDR-corrected p = 0.006 across the five-term spectral family; adjusted R^2 = 0.22) (**Fig. 3E**) (see **Table S1**).

As a secondary analysis, we refitted the full coupling model across all six electrode groups, both eyes-open and eyes-closed conditions, and three spectral fitting ranges (1 to 35, 1 to 40, 1 to 45 Hz), both to confirm robustness to spectral-parameterization and regional choices and to test whether the coupling was specific to the eyes-open condition. The eyes-open exponent relationship was negative in every case, with 8 of the 108 cells surviving correction, all in the eyes-open condition for mean reaction time (**Fig. S2A**). In the eyes-closed condition, the exponent to mean reaction time coupling was absent across all six electrode groups and all three fitting ranges. A condition-by-exponent interaction confirmed the coupling differed between conditions (β = 65.60, 95% CI [26.26, 104.93], corrected p = 0.002 across the two interaction contrasts), with within-condition estimates of -91.11 ms eyes-open and 4.04 ms eyes-closed (p = 0.854). The coupling was not moderated by baseline age and did not depend on the follow-up interval, and baseline reaction time remained the only significant covariate (all other terms p > 0.05). Furthermore, although the exponent effect was regionally broad, it was not always the only spectral change to track slowing. Repeating the joint spectral model across the same condition, region and fitting-range grid, the change in the exponent was the most consistent and widely distributed spectral predictor of slowing under eyes-open but not eyes-closed recording. Some aperiodic-adjusted peak-power changes showed effects that were only locally over occipital electrodes (alpha and beta in eyes-open condition; delta, in eyes-closed condition) (**Fig. S2B**).

Simon task response times slow and 'No-Go' accuracy improves in neurotypical adults

JNeurosci Accepted Manuscript

We next characterized the longitudinal change in executive function, assayed by a modified Simon task across three measures: mean 'Go' response time, the Simon effect (incongruent minus congruent response time) indexing interference control, and 'No Go' accuracy indexing response inhibition (**Fig. 4A**). Within individuals, mean 'Go' response time increased from baseline to follow-up (mean change = 12.397 ms, 95% CI [4.549, 20.244]; permutation sign-flip test raw p = 0.002, corrected p = 0.003, paired t(221) = 3.09, dz = 0.21), however the Simon effect did not change (mean change = 1.163 ms, 95% CI [-2.243, 4.569], permutation sign-flip test corrected p = 0.499, dz = 0.04). In contrast, 'No Go' accuracy improved (mean change = 0.029, 95% CI [0.014, 0.044]; permutation sign-flip test corrected p < 1 x 10-4, paired t(221) = 3.68, dz = 0.25) **(Fig. 4B-D)**. Linear mixed-effects models of each measure (*measure ~ session + age + sex + (1 | participant)*) confirmed these within-person changes and separated them from the between-person age gradient. Cross-sectionally, older baseline age was associated with slower response time (β = 2.227 ms per year, 95% CI [1.411, 3.042], corrected p < 0.001), a larger Simon effect (β = 0.448 ms per year, 95% CI [0.195, 0.700], corrected p < 0.001), and a modest reduction in no-go accuracy (β = -0.001 per year, 95% CI [-0.002, 0.000], corrected p = 0.053) **(Fig. 4E-G)**. Taken together, there is a clear dissociation across measures such that response times slowed both within individuals and across the cross-sectional age range. While the Simon effect carried a cross-sectional age gradient there was no within-person change, and yet 'No-Go' accuracy improved within individuals despite a marginal cross-sectional decline with age (**Fig. 4H-J**) (see **Table S1**).

We then confirmed that the two within-person changes were not artifacts of baseline-dependent change or session interval. For mean 'Go' response time, baseline performance predicted the magnitude of change (β = -0.213, 95% CI [-0.30, -0.13], p < 0.001) (**Fig. S3A**), consistent with regression to the mean. Yet the slowing survived adjustment for baseline level (intercept at the mean baseline = 10.8 ms, 95% CI [1.05, 20.60], p = 0.03) and, unlike the cohort-wide PVT

JNeurosci Accepted Manuscript

slowing, was concentrated in older participants, with this age relationship persisting after residualizing on baseline performance, sex and follow-up interval (β = 1.23 ms per year, 95% CI [0.64, 1.82], p < 0.001) (**Fig. S3B**). 'No Go' accuracy likewise showed regression to the mean (β = -0.617, p < 0.001, adjusted R^2 = 0.37) (**Fig. S3C**) and survived baseline adjustment (intercept = 0.030, p < 0.001), but this improvement carried only a modest residual age relationship, such that older participants improved slightly less (β = -0.001 per year, 95% CI [-0.002, 0.000], p = 0.034) (**Fig. S3D**).

The aperiodic exponent does not track concurrent Simon task measures

We next investigated whether the aperiodic exponent was correlated with Simon task performance, taking mean 'Go' response time as the executive-function analogue of PVT mean reaction time since it also slowed within individuals (**Fig. 4**). Across the pooled baseline and follow-up sessions, 'Go' response time did not correlate with the exponent (β = 16.7 ms per unit, 95% CI [-29.70, 63.04], uncorrected p = 0.48; within-session baseline r = -0.06, follow-up r = -0.17) and, unlike the PVT, the slope relating the exponent to response time did not change at follow-up (exponent x session, β = -43.0 ms, 95% CI [-95.65, 9.70], uncorrected p = 0.11) (**Fig. 5A).** Within individuals, exponent change was unrelated to change in mean 'Go' response time (r(220) = -0.02, p = 0.78) (**Fig. 5B**), and baseline exponent likewise did not predict mean 'Go' response time change (r(220) = -0.03, p = 0.69) (**Fig. 5C**). In a multivariable model that included the change and the baseline exponent simultaneously, together with baseline age, baseline response time, sex and the follow-up interval, the exponent effect was absent (*Δexponent*, β = -15.2 ms, 95% CI [-71.69, 41.21], raw p = 0.595, FDR-corrected p = 0.965; adjusted R^2 = 0.15) **(Fig. 5D).** The same model recovered the previously observed structure: 'Go' mean response time slowing was concentrated in older participants (*age*, β = 1.3 ms per year, 95% CI [0.68, 1.99], p < 0.001) and baseline 'Go' mean response time negatively related to its own change (β

JNeurosci Accepted Manuscript

= -0.26, p < 0.001), consistent with regression to the mean. These results collectively confirm that the absent exponent effect was not an artifact of a model unable to recapitulate our prior observations. This null held across all six electrode groups, both recording conditions and three fitting ranges, with no surviving correction in any configuration (**Fig. S4**). Applied to the remaining Simon measures, the same model was likewise null after correction. The exponent did not track the Simon effect (*Δexponent*, β = -3.1, FDR-corrected p = 0.990) (**Fig. 5E**) nor 'No Go' accuracy (*Δexponent*, β = 0.084, FDR-corrected p = 0.965) (**Fig. 5F**). Thus, in contrast to the PVT, the within-person exponent change was uncoupled from every Simon measure (see **Table S1**).

Aperiodic exponent decline carries a stable, state- and domain-specific predictive signal for attentional slowing

The mixed-effects model results that we previously observed (**Fig. 3**) were estimated in a single sample, so we next asked whether it was stable, state-specific, and behaviorally specific. We thus refitted the model across 200 age-stratified 80/20 cross-validation splits of the training set (n = 222; n = 220 for post-task models, two participants each lacking a post-task eyes-open recording at one session). We used these repeated within-training splits to assess stability, reserving the frozen test set (n = 54) as the single independent generalization test.

Using pre-task data, the coefficient relating exponent change to PVT mean reaction time change was negative in every resample (i.e., a steeper exponent decline predicted greater slowing; median -93.46 ms per unit), and its sign agreed between the model-fitting and held-out partitions of each split in 93% of resamples (single-partition training estimate β = -91.11 ms, p < 0.001) (**Fig. 6A**) (see **Table S2**). The post-task coefficient, in contrast, was centered near zero with an unstable sign (median -2.08 ms, negative in 56.5% of resamples, partition concordance

JNeurosci Accepted Manuscript

16%), indicating that the stable relationship present in pre-task EEG was absent in post-task EEG. An acquisition-by-exponent interaction confirmed this difference (β = 54.65, 95% CI [18.97, 90.34], corrected p = 0.003 across the two interaction contrasts, n = 220), with within-acquisition estimates of -90.45 ms pre-task and -2.92 ms post-task (p = 0.897). To further explore whether this was due to state-specificity (e.g., cognitive or attentional fatigue over the entirety of the experiment), we tested the held-out prediction of the PVT change and found that both models predicted above zero in the majority of resamples (pre-task median held-out R^2 = 0.167, root-mean-squared error = 51.1 ms, positive in 84% of resamples; post-task median held-out R2 = 0.122, root-mean-squared error = 52.0 ms, positive in 74%) (**Fig. 6B**). However, both were largely driven by baseline reaction time (see **Fig. 3D**), suggesting that regression to the mean inflated this marginal R^2 and thus obscured the exponent's specific contribution.

To remove that shared component, we took the paired difference in held-out R^2 between the pre-task and post-task models fitted on the same 220 participants. This pre-minus-post increment was positive (median across resamples 0.058, mean 0.053, 2.5th-97.5th percentile spread [-0.078, 0.162]), and its mean exceeded a full label-shuffle null (observed mean ΔR^2 = 0.052; null mean = -0.001, SD = 0.018; two-sided permutation test, 1,000 global permutations x 100 folds, p = 0.008) (**Fig. 6C**), indicating a modest, reliable predictive advantage of pre-task over post-task EEG for the PVT change relationship. We then asked whether state-specificity also manifested at the level of feature use. We fitted a penalized (elastic-net) model and expressed the exponent weight on a common scale across sessions (standardized by the outcome's standard deviation). The pre-task exponent carried a consistent negative standardized weight (median -0.235), whereas the post-task weight was approximately zero, and the weights were retained under the L1 penalty in 100% and 12% of resamples respectively **(Fig. 6D).** Placing the exponent weight on a common scale, the pre-task exponent predicting change in Simon 'Go' response time was negligible (median standardized weight approximately

JNeurosci Accepted Manuscript

0) in contrast to the pre-task PVT weight (median -0.235), and the two were retained under the L1 penalty in 28% and 100% of resamples respectively, suggesting a domain dissociation.

We then evaluated the *a priori* held-out set (n = 54) as the single independent test of generalizability (**Fig. 1A**). Refitting the coupling model within the held-out set returned a non-significant, positive coefficient (β = 1.416 ms, p = 0.98), and applying the frozen training model to predict held-out PVT change gave a negative out-of-sample R^2 (-0.181), indicating a prediction worse than the held-out sample mean. These fell at the 93rd and 2.5th percentiles, respectively, of the resample distribution **(Fig. 6E)**. The coefficient being in the upper tail of the distribution (where the held-out coefficient flips sign) combined with an R^2 near the bottom suggests an underpowered draw, since cross-validated estimates carry large sampling variance at small sample sizes (Varoquaux, 2018). Thus, our one fully independent test did not confirm out-of-sample prediction, and we therefore present generalization as supported by coefficient stability within the training sample only.

Repeating the full analysis with folds stratified jointly on age and baseline mean response time (in place of age alone) led to similar findings: the pre-task coefficient remained negative in 100% of resamples (median -91.88 ms, concordance 100%), the paired predictive increment was again significant yet modest (observed mean ΔR^2 = 0.056, two-sided permutation p = 0.014), and the standardized exponent weights reproduced the same state and domain dissociations (PVT pre-task median standardized weight = -0.232, retained in 100% of resamples; PVT post-task median standardized weight approximately 0, retained in 12.5% of resamples; Simon pre-task median standardized weight approximately 0, retained in 22.5% of resamples) (**Fig. S5**).

Discussion

JNeurosci Accepted Manuscript

Our analyses asked whether within-person changes in the task-free EEG aperiodic exponent track concurrent cognitive-behavioral changes across aging, and whether any such coupling is generalizable across cognitive-behavioral domains. We found that the aperiodic exponent declined within individuals over an approximately five-year follow-up interval, separably from the age at baseline and from concurrent changes in aperiodic adjusted oscillatory-power, and robustly across spectral parameterization fitting ranges and electrode regions. In parallel, PVT mean reaction time slowed over the same interval, reflecting age-related decline in sustained attention and processing speed, while reaction-time variability and accuracy did not change. Our central finding is that the within-person exponent decline tracked concurrent PVT slowing after adjusting for multiple covariates, including baseline age and performance, and was specific to the aperiodic exponent rather than to oscillatory features. By contrast, no exponent relationship emerged for any Simon-task measure despite behavioral changes in that domain, including 'Go' response time slowing and 'No-Go' accuracy improvements, suggesting a cognitive-behavioral domain dissociation. Our predictive modeling analyses showed that the exponent decline and PVT slowing coupling was stable across resamples, was state-specific (pre-task over post-task EEG), and was domain-specific (PVT over Simon task performance). Overall, our findings suggest that the age-related aperiodic exponent decline indexes attentional and processing-speed performance rather than general cognitive-behavioral aging, even within a time interval as short as five years.

Prior cross-sectional work established that the slope of the EEG power spectrum in log-log space 'flattens' with neurotypical aging (i.e., the aperiodic exponent decreases) (Voytek et al., 2015; Dave et al., 2018; Merkin et al., 2023). An independent study drawing on the same cohort we analyzed (the Dortmund Vital Study; Gajewski et al., 2022; Getzmann et al., 2024) similarly showed that the exponent declines over an average of five years in neurotypical adults (Politanskaia et al., 2026). Here, we extend these findings as the first to show that within-person

JNeurosci Accepted Manuscript

753 change in the aperiodic exponent tracks concurrent cognitive-behavioral change within the
754 same individuals, and report that this coupling may be dissociated from cross-sectional age
755 relationships. For instance, the between-person age gradient sometimes existed without a
756 corresponding within-person change. In our data the Simon effect carried a reliable age gradient
757 ($\beta = 0.448$ ms per year, corrected $p < 0.001$) but showed no longitudinal change across the
758 interval (1.163 ms, corrected $p = 0.504$). This dissociation aligns with findings from the largest
759 cross-sectional study of aperiodic activity and cognitive aging to date, in which the exponent
760 declined with age across more than 1700 older adults (Cesnaite et al., 2023). That study found
761 no reliable association with cognition, including a processing-speed factor indexed by the Stroop
762 test (Cesnaite et al., 2023). Similarly, the baseline exponent did not predict PVT change (**Fig.**
763 **3C**). These dissociations caution against inferring within-person aging trajectories from cross-
764 sectional age effects in studies of aperiodic neural activity and cognition.
765
766 The within-person exponent decline tracked PVT slowing but not any change in Simon-task
767 measures, including 'Go' response time, which, while it slowed longitudinally, remained
768 uncoupled. This suggests that the exponent tracks the specific attentional-speed demands of
769 the PVT rather than general RT slowing. But executive function also recruits information
770 processing, so one possibility, which our work does not directly test, is that the aperiodic
771 exponent tracks the speed or efficiency of information processing shared across cognitive-
772 behavioral tasks, rather than interference control itself. For example, a 'flatter' spectral slope in
773 older adults is linked to less consistent stimulus-evoked responses in a visual attention task
774 (Tran et al., 2020) and to sustained attention specifically (Campbell et al., 2024). Furthermore,
775 cross-sectional work has shown that the aperiodic exponent relates to some cognitive domains
776 more than others (McKeown et al., 2025; Campbell et al., 2026), so a domain-specific coupling
777 may not be atypical. Beyond the tasks analyzed here, the broader Dortmund Vital Study
778 (Gajewski et al., 2022) includes assessments that could provide further insight into these

JNeurosci Accepted Manuscript

findings, such as the AX-continuous performance task, an auditory distraction task, and a visual search task of spatial selective attention. For example, the AX-continuous performance task varies attentional demand across cue-probe combinations. If the exponent-behavior coupling we observed generally reflects processing speed, regardless of task, then this coupling would be present and uniform across those conditions, whereas a coupling that reflects attentional control would not. These assessments were not part of the data transfer used in our analyses, but they offer clear next steps for determining whether exponent coupling reflects processing speed shared across tasks or attention-specific demands.

The coupling between the aperiodic exponent and PVT reaction time was carried by pre-task, but not post-task, EEG (**Fig. 6A, D**) and was present in the eyes-open, but not eyes-closed, condition (**Fig. S2A**). It may be that EEG collected before any task is reflective of a rested baseline that is more predictive of subsequent behavior, whereas EEG after the task could be contaminated by task-induced fatigue and general shifts in arousal (Lendner et al., 2020; Cunningham et al., 2023). The pre-minus-post-task predictive increment reached significance against a full label-shuffle null (observed mean $\Delta R^2 = 0.052$, $p = 0.008$) (**Fig. 6C**). This was further supported by a coupling coefficient that was sign-stable in 100% of resamples, and by a consistently negative pre-task exponent weight against a post-task weight of approximately zero, consistent with state-specific exponent-PVT mRT coupling.

A limitation in interpreting our results stems from the observational and correlational nature of our findings. We therefore cannot establish that exponent decline causes attentional slowing, as both may arise from upstream disruptions found in healthy aging, such as neurodegeneration or vascular changes. Aperiodic activity is also a complex measure with many neural and non-neural contributors (Fitzgerald et al., 2024; Preston et al., 2026). Most notably, cardiac activity can survive ICA-based correction and has been shown to influence aperiodic exponent

JNeurosci Accepted Manuscript

estimates (Schmidt et al., 2024). However, such confounds should track behavior irrespective of cognitive domain, recording state, or eyes condition. Our observed coupling was specific to the PVT, to pre-task EEG, and to the eyes-open condition, suggesting that the coupling is not reducible to non-neural contributions. Furthermore, spectral model fits were comparable or marginally better in eyes-closed recordings, so the absence of coupling in that condition cannot be attributed to worse parameterization (see Methods). With regards to our *a priori* held-out test set, the refitted coefficient was positive and non-significant ($\beta = 1.416$, $p = 0.98$), sitting at the 93rd percentile of the resample distribution, while the out-of-sample R^2 was negative (-0.181) at the 2.5th percentile (**Fig. 6E**), suggesting an atypical, low-powered draw rather than a clear null, though generalization to the independent set was not confirmed. Our generalization claims therefore rest on the resampling distribution and feature-weight analyses.

An additional challenge in interpreting our findings is that the healthy-volunteer cohort produced a counterintuitive between-person age effect, with older participants faster at baseline on PVT reaction time **(Fig. 2D, E).** Although this gradient did not survive multiple-comparison correction, its direction may reflect an inherent recruitment bias toward healthier and more cognitively able older adults in studies of this kind, limiting generalization to clinical or at-risk populations. Furthermore, education has been shown to moderate the cross-sectional relationship between the aperiodic exponent and cognition (Montemurro et al., 2024). Education may be more likely a moderator of the rate of change than a confound of the coupling itself, though with only two timepoints we cannot characterize the trajectory's shape, non-linearity, or heterogeneity in the rate of change across our measures. Finally, our reported effect sizes were modest (d_z values of approximately 0.2 to 0.3) and the exponent's incremental predictive contribution beyond baseline covariates was small in absolute terms. With only two cognitive-behavioral domains tested, there remains a clear need to delineate what the aperiodic exponent does and does not track and whether any changes are advantageous to daily life tasks.

JNeurosci Accepted Manuscript

Our study shows that within-person exponent changes track concurrent cognitive-behavioral changes, positioning the aperiodic exponent as a longitudinal, within-person neural biomarker of attentional slowing rather than a cross-sectional correlate. The exponent is widely interpreted as an index of cortical excitation-inhibition balance, such that a flatter spectrum reflects a shift toward excess excitation and reduced inhibition with age (Voytek et al., 2015; Gao et al., 2017). While we do not test that framework here, we provide a foundation for pairing aperiodic exponent measures with more direct indices of synaptic and neurotransmitter tone, such as its reported relationship to glutamatergic signaling (Sheldon et al., 2026), to track changes in attentional performance in model organisms. Future work should extend these findings to at-risk cohorts, use a denser longitudinal sampling to model individual trajectories, broaden the cognitive battery to map the boundaries of aperiodic neural activity coupling, and combine the exponent with complementary, multimodal biomarkers such as white-matter microstructure. Finally, transcranial random aperiodic stimulation has been shown to improve working memory precision when the exponent is increased, which is opposite to the aging-related decline we observed, raising the possibility of testing whether the attentional slowing in aging populations is directly manipulable (van Engen et al., 2026).

References

Agüero-Torres H, Thomas VS, Winblad B, Fratiglioni L (2002) The impact of somatic and cognitive disorders on the functional status of the elderly. J Clin Epidemiol 55:1007–1012.

JNeurosci Accepted Manuscript

Antúnez M, McSweeney M, Zeytinoglu S, Tan E, Zeanah CH, Nelson CA, Fox NA (2025) Exploring background aperiodic electroencephalography (EEG) activity in the Bucharest Early Intervention Project. Developmental Psychology 61:1371–1383.

Avila CG, May ES, Bott FS, Tiemann L, Hohn V, Heitmann H, Zebhauser PT, Gross J, Ploner M (2024) Assessing the balance between excitation and inhibition in chronic pain through the aperiodic component of EEG. eLife 13

Baddeley AD, Baddeley HA, Bucks RS, Wilcock GK (2001) Attentional control in Alzheimer's disease. Brain 124:1492–1508.

Baddeley AD, Bressi S, Della Sala S, Logie R, Spinnler H (1991) The decline of working memory in Alzheimer's disease. A longitudinal study. Brain 114 (Pt 6):2521–2542.

Benjamini Y, Hochberg Y (1995) Controlling the False Discovery Rate: A Practical and Powerful Approach to Multiple Testing. Royal Statistical Society Journal Series B: Methodological 57:289–300

Brake N, Duc F, Rokos A, Arseneau F, Shahiri S, Khadra A, Plourde G (2024) A neurophysiological basis for aperiodic EEG and the background spectral trend. Nat Commun 15:1514.

Buzsáki G, Anastassiou CA, Koch C (2012) The origin of extracellular fields and currents — EEG, ECoG, LFP and spikes. Nat Rev Neurosci 13:407–420 Available at: https://www.nature.com/articles/nrn3241

Campbell AJ, Anijärv TE, Johansson M, Pace T, Lagopoulos J, Hermens DF, Levenstein JM, Andrews SC (2026) Resting-state EEG aperiodic exponent moderates the association between age and memory performance in older adults. Neurobiol Aging 160:10–21.

Campbell AJ, Anijärv TE, Pace T, Treacy C, Lagopoulos J, Hermens DF, Levenstein JM, Andrews SC (2024) Resting-state EEG correlates of sustained attention in healthy

JNeurosci Accepted Manuscript

878 ageing: Cross-sectional findings from the LEISURE study. Neurobiology of Aging
879 144:68–77

880 Cesnaite E, Steinfath P, Jamshidi Idaji M, Stephani T, Kumral D, Haufe S, Sander C, Hensch T,
881 Hegerl U, Riedel-Heller S, Röhr S, Schroeter ML, Witte AV, Villringer A, Nikulin VV
882 (2023) Alterations in rhythmic and non-rhythmic resting-state EEG activity and their link
883 to cognition in older age. Neuroimage 268:119810.

884 Chakravarty K, Roy S, Sinha A, Kumar A (2025) Can we infer excitation-inhibition balance from
885 the spectrum of population activity? Commun Biol 9:51

886 Chini M, Pfeffer T, Hanganu-Opatz I (2022) An increase of inhibition drives the developmental
887 decorrelation of neural activity de la Prida LM, Colgin LL, Vanhatalo S, eds. eLife
888 11:e78811

889 Cunningham E, Zimnicki C, Beck DM (2023) The Influence of Prestimulus 1/f-Like versus Alpha-
890 Band Activity on Subjective Awareness of Auditory and Visual Stimuli. J Neurosci
891 43:6447–6459.

892 Dave S, Brothers TA, Swaab TY (2018) 1/f neural noise and electrophysiological indices of
893 contextual prediction in aging. Brain Res 1691:34–43.

894 Dinges DF, Powell JW (1985) Microcomputer analyses of performance on a portable, simple
895 visual RT task during sustained operations. Behavior Research Methods, Instruments, &
896 Computers 17:652–655

897 Donoghue T, Haller M, Peterson EJ, Varma P, Sebastian P, Gao R, Noto T, Lara AH, Wallis JD,
898 Knight RT, Shestyuk A, Voytek B (2020) Parameterizing neural power spectra into
899 periodic and aperiodic components. Nat Neurosci 23:1655–1665

JNeurosci Accepted Manuscript

Donoghue T, Schaworonkow N, Voytek B (2022) Methodological Considerations for Studying Neural Oscillations. Eur J Neurosci 55:3502–3527

Erb CD, Germine L, Hartshorne JK (2023) Cognitive control across the lifespan: Congruency effects reveal divergent developmental trajectories. Journal of Experimental Psychology: General 152:3285–3291.

Finley AJ, Angus DJ, Knight EL, van Reekum CM, Lachman ME, Davidson RJ, Schaefer SM (2024) Resting EEG Periodic and Aperiodic Components Predict Cognitive Decline Over 10 Years. J Neurosci 44:e1332232024

Fitzgerald M, Kosik E, Voytek B (2024) Unveiling hidden sources of noise. Elife 13:e102878.

Fjell AM, Walhovd KB, Fischl B, Reinvang I (2007) Cognitive function, P3a/P3b brain potentials, and cortical thickness in aging. Hum Brain Mapp 28:1098–1116

Fortenbaugh FC, DeGutis J, Germine L, Wilmer JB, Grosso M, Russo K, Esterman M (2015) Sustained Attention Across the Life Span in a Sample of 10,000: Dissociating Ability and Strategy. Psychol Sci 26:1497–1510.

Gajewski PD, Getzmann S, Bröde P, Burke M, Cadenas C, Capellino S, Claus M, Genç E, Golka K, Hengstler JG, Kleinsorge T, Marchan R, Nitsche MA, Reinders J, van Thriel C, Watzl C, Wascher E (2022) Impact of Biological and Lifestyle Factors on Cognitive Aging and Work Ability in the Dortmund Vital Study: Protocol of an Interdisciplinary, Cross-sectional, and Longitudinal Study. JMIR Res Protoc 11:e32352.

Gao R, Peterson EJ, Voytek B (2017) Inferring synaptic excitation/inhibition balance from field potentials. NeuroImage 158:70–78

JNeurosci Accepted Manuscript

Gao R, van den Brink RL, Pfeffer T, Voytek B (2020) Neuronal timescales are functionally dynamic and shaped by cortical microarchitecture. Elife 9:e61277.

Getzmann S, Gajewski PD, Schneider D, Wascher E (2024) Resting-state EEG data before and after cognitive activity across the adult lifespan and a 5-year follow-up. Sci Data 11:988

Gramfort A, Luessi M, Larson E, Engemann DA, Strohmeier D, Brodbeck C, Parkkonen L, Hämäläinen MS (2014) MNE software for processing MEG and EEG data. Neuroimage 86:446–460.

Harris CR et al. (2020) Array programming with NumPy. Nature 585:357–362.

He BJ (2014) Scale-free brain activity: past, present, and future. Trends in Cognitive Sciences 18:480–487

Hoppe K, Küper K, Wascher E (2017) Sequential Modulations in a Combined Horizontal and Vertical Simon Task: Is There ERP Evidence for Feature Integration Effects? Front Psychol 8

Hugo J, Ganguli M (2014) Dementia and Cognitive Impairment: Epidemiology, Diagnosis, and Treatment. Clin Geriatr Med 30:421–442

Hunter JD (2007) Matplotlib: A 2D Graphics Environment. Comput Sci Eng 9:90–95

Jas M, Engemann DA, Bekhti Y, Raimondo F, Gramfort A (2017) Autoreject: Automated artifact rejection for MEG and EEG data. Neuroimage 159:417–429.

Lanzone J, Colombo MA, Sarasso S, Zappasodi F, Rosanova M, Massimini M, Di Lazzaro V, Assenza G (2022) EEG spectral exponent as a synthetic index for the longitudinal assessment of stroke recovery. Clin Neurophysiol 137:92–101.

JNeurosci Accepted Manuscript

Lejko N, Larabi DI, Herrmann CS, Aleman A, Ćurčić-Blake B (2020) Alpha Power and Functional Connectivity in Cognitive Decline: A Systematic Review and Meta-Analysis. J Alzheimers Dis 78:1047–1088.

Lendner JD, Helfrich RF, Mander BA, Romundstad L, Lin JJ, Walker MP, Larsson PG, Knight RT (2020) An electrophysiological marker of arousal level in humans Haegens S, Colgin LL, Piantoni G, eds. eLife 9:e55092

Li A, Feitelberg J, Saini AP, Höchenberger R, Scheltienne M (2022) MNE-ICALabel: Automatically annotating ICA components with ICLabel in Python. Journal of Open Source Software 7:4484

Li N, Yang J, Long C, Lei X (2024) Test-Retest Reliability of EEG Aperiodic Components in Resting and Mental Task States. Brain Topogr 37:961–971.

Marinazzo D (2026) From periodic/aperiodic to static/dynamic: rethinking the decomposition of neural power spectra. :2026.07.26.740811 Available at: https://www.biorxiv.org/content/10.64898/2026.07.26.740811v1

McKeown DJ, Roberts E, Finley AJ, Kelley NJ, Keage HAD, Schinazi VR, Baumann O, Moustafa AA, Angus DJ (2025) Lower aperiodic EEG activity is associated with reduced verbal fluency performance across adulthood. Neurobiol Aging 151:29–41.

McSweeney M, Morales S, Valadez EA, Buzzell GA, Fox NA (2021) Longitudinal age- and sex-related change in background aperiodic activity during early adolescence. Dev Cogn Neurosci 52:101035

JNeurosci Accepted Manuscript

962 Merkin A, Sghirripa S, Graetz L, Smith AE, Hordacre B, Harris R, Pitcher J, Semmler J,
963 Rogasch NC, Goldsworthy M (2023) Do age-related differences in aperiodic neural
964 activity explain differences in resting EEG alpha? Neurobiology of Aging 121:78–87

965 Miller KJ (2010) Broadband Spectral Change: Evidence for a Macroscale Correlate of
966 Population Firing Rate? J Neurosci 30:6477–6479

967 Montemurro S, Borek D, Marinazzo D, Zago S, Masina F, Napoli E, Filippini N, Arcara G (2024)
968 Aperiodic component of EEG power spectrum and cognitive performance are modulated
969 by education in aging. Sci Rep 14:15111

970 Park J, Ho RLM, Wang W-E, Nguyen VQ, Coombes SA (2024) The effect of age on alpha
971 rhythms in the human brain derived from source localized resting-state
972 electroencephalography. Neuroimage 292:120614.

973 Pion-Tonachini L, Kreutz-Delgado K, Makeig S (2019) ICLabel: An automated
974 electroencephalographic independent component classifier, dataset, and website.
975 NeuroImage 198:181–197

976 Politanskaia P, Bywater J, Finley AJ, Keage HAD, Kelley NJ, McKeown DJ, Schinazi VR, Angus
977 DJ (2026) Long-term reliability and stability of parameterized resting state EEG:
978 evidence from a five-year follow-up. Cereb Cortex 36:bhag113

979 Pré D, Cazares C, Wooten AT, Zhou H, Onofre I, Neil A, Logan T, Hu R, Lui JH, Voytek B, Bang
980 AG (2026) Pharmacological manipulation of nested oscillations in human iPSC-derived
981 2D neuronal networks. Neurobiology of Disease 220:107281

982 Preston M, Smith S, Voytek B (2026) Potential mechanisms and functional significance of
983 aperiodic neural activity. Nat Hum Behav.

JNeurosci Accepted Manuscript

Ranasinghe KG, Kudo K, Casaletto K, Rojas-Martinez JC, Syed F, Vossel K, Miller BL, Rabinovici GD, Kramer JH, Rankin KP, Nagarajan SS (2025) Neurophysiological signatures of ageing: compensatory and compromised neural mechanisms. Brain Commun 7:fcaf131

Roberts, A. W., Ogunwole, S. U., Blakeslee, L. & Rabe, M. A. (2018) The Population 65 Years and Older in the United States. Census.gov

Salvatore SV, Lambert PM, Benz A, Rensing NR, Wong M, Zorumski CF, Mennerick SJ (2024) Periodic and aperiodic changes to cortical EEG in response to pharmacological manipulation. J Neurophysiol.

Schmidt F, Danböck SK, Trinka E, Klein DP, Demarchi G, Weisz N (2024) Age-related changes in “cortical” 1/f dynamics are linked to cardiac activity. eLife 13

Sheldon AA, Moser HR, Abdullahi KS, Allison KD, Mulder CB, Montoya SA, Sponheim SR, Marjańska M, Schallmo M-P (2026) Aperiodic slope reflects glutamatergic tone in the human brain. Brain Res 1874:150161.

Simon JR (1969) Reactions toward the source of stimulation. Journal of Experimental Psychology 81:174–176.

Skipper S, Perktold J (2010) Statsmodels: Econometric and Modeling with Python. 9th Python in Science Conference, Austin, 28 June-3 July, 2010, 57-61.

Smith SE, Ma V, Gonzalez C, Chapman A, Printz D, Voytek B, Soltani M (2023) Clinical EEG slowing induced by electroconvulsive therapy is better described by increased frontal aperiodic activity. Transl Psychiatry 13:348.

JNeurosci Accepted Manuscript

Tran TT, Rolle CE, Gazzaley A, Voytek B (2020) Linked Sources of Neural Noise Contribute to Age-related Cognitive Decline. J Cogn Neurosci 32:1813–1822.

Uudeberg T, Päeske L, Hinrikus H, Lass J, Põld T, Bachmann M (2025) Individual stability of single-channel EEG measures over one year in healthy adults. Sci Rep 15:28426

Vallesi A, Tronelli V, Lomi F, Pezzetta R (2021) Age differences in sustained attention tasks: A meta-analysis. Psychon Bull Rev 28:1755–1775.

van Dinteren R, Arns M, Jongsma MLA, Kessels RPC (2014) P300 Development across the Lifespan: A Systematic Review and Meta-Analysis. PLoS One 9:e87347

van Engen Q, Riddle J, Voytek B (2026) Transcranial Random Aperiodic Stimulation Improves Working Memory Precision. :2026.09.08.750163 Available at: https://www.biorxiv.org/content/10.64898/2026.09.08.750163v1 [Accessed September 17, 2026].

Varoquaux G (2018) Cross-validation failure: Small sample sizes lead to large error bars. Neuroimage 180:68–77.

Voytek B, Knight RT (2015) Dynamic network communication as a unifying neural basis for cognition, development, aging, and disease. Biol Psychiatry 77:1089–1097.

Voytek B, Kramer MA, Case J, Lepage KQ, Tempesta ZR, Knight RT, Gazzaley A (2015) Age-Related Changes in 1/f Neural Electrophysiological Noise. J Neurosci 35:13257–13265.

Wang Z, Yang S, Lu J, Zhou Q (2026) Reliable and dynamic monitoring changes in cortical excitation and inhibition balance using aperiodic 1/f slope: functions, diseases and drug effects. Neuroscience 595:9–19.

JNeurosci Accepted Manuscript

Wascher E, Sharifian F, Gutberlet M, Schneider D, Getzmann S, Arnau S (2022) Mental chronometry in big noisy data. PLOS ONE 17:e0268916

Waskom ML (2021) seaborn: statistical data visualization. Journal of Open Source Software 6:3021

Wiest C, Torrecillos F, Pogosyan A, Bange M, Muthuraman M, Groppa S, Hulse N, Hasegawa H, Ashkan K, Baig F, Morgante F, Pereira EA, Mallet N, Magill PJ, Brown P, Sharott A, Tan H (2023) The aperiodic exponent of subthalamic field potentials reflects excitation/inhibition balance in Parkinsonism Swann NC, de Lange FP, Voytek B, eds. eLife 12:e82467

Wilkinson CL, Yankowitz LD, Chao JY, Gutiérrez R, Rhoades JL, Shinnar S, Purdon PL, Nelson CA (2024) Developmental trajectories of EEG aperiodic and periodic components in children 2–44 months of age. Nat Commun 15:5788

Author Contributions

C.C. designed research, analyzed data, and wrote the first draft of the paper; A.R. and L.K. analyzed data and edited the paper; S.G., S.A., and E.W. performed research and edited the paper; B.V. designed research and edited the paper; C.C., A.R., L.K., S.G., S.A., E.W., and B.V. wrote the paper.

JNeurosci Accepted Manuscript

Figure Legends

Figure 1. The aperiodic exponent declines within neurotypical adults.

(A) Study design. Sessions were identical at baseline and at the approximately five-year follow-up: pre-task EEG (eyes closed then eyes open), a cognitive test battery that included the PVT and Simon tasks analyzed here, then post-task EEG. **(B)** Baseline age distribution by sex for the training (blue, n = 222) and held-out test (grey, n = 54) sets. Split violins mark quartiles with individual participants overlaid. The sets did not differ in baseline age (Mann-Whitney U = 5,864, p = 0.80) or sex (chi-squared test, $\chi^2(1) = 0.39$, p = 0.53). **(C)** Group power spectra plotted in log-log space at baseline (teal) and follow-up (orange) with the aperiodic fit overlaid (dashed). Lines and shading show the mean and ±1 standard deviation for all electrodes across participants. **(D)** Within-person exponent change (follow-up minus baseline) under eyes-open and eyes-closed conditions. Clouds show the participant distribution and the point and whisker show the mean and its 95% confidence interval. The exponent declined in both conditions (eyes open mean = -0.040; eyes closed mean = -0.045; two-sided sign-flip permutation test, 10,000 permutations, Benjamini-Hochberg corrected across the two recording conditions; eyes open corrected $p = 1 \times 10^{-4}$, eyes closed corrected $p < 1 \times 10^{-4}$) and the decline did not differ between conditions (sign-flip permutation, paired t(221) = 0.46, p = 0.64). **(E)** Scalp topography of the mean exponent change across 64 channels (eyes-open condition). **(F)** Exponent against age at baseline (teal) and follow-up (orange) with mixed-effects lines overlaid (all electrodes mean, eyes-open condition). Line slope is the between-person age gradient and the offset between lines indicates the within-person change. **(G)** Mixed-effects coefficients for exponent level from the same model: within-person change (β = -0.040), baseline age (β = -0.0053 per year), and sex (β = +0.026). The change and age terms survived correction across the two recording conditions (both corrected p < 0.001); sex did not differ from zero (p = 0.29, uncorrected). Error

JNeurosci Accepted Manuscript

bars are 95% confidence intervals with significant terms in blue and non-significant in grey. **(H)** Coefficients relating concurrent band-power change to exponent change (all electrodes mean, eyes-open condition). No band predicted the decline (ordinary least-squares regression, Benjamini-Hochberg FDR across the four-band Δ-power family; all FDR-corrected $p > 0.05$, with ΔDelta closest at corrected $p = 0.056$**). (I)** Within-person change coefficient (linear mixed-effects model) across three spectral parameterization fitting ranges and six electrode groups. The coefficient was negative in all 18 cells; shading denotes the Benjamini-Hochberg corrected p across this 18-cell robustness grid and asterisks mark cells surviving correction (17 of 18; the exception is the central region at 1-45 Hz, $\beta = -0.009$, corrected $p = 0.376$). n = 276 in B, n = 222 (training set) in C to H, n = 220-222 in I, varying by region and fitting range with the number of participants retaining at least two channels meeting the $R^2 \geq 0.90$ criterion**.** † < 0.07, *p < 0.05, **p < 0.01, ***p < 0.001.

Figure 2. Reaction time in the PVT slows within neurotypical adults.

(A) Schematic of the psychomotor vigilance task. After a variable interstimulus interval (ISI) of 2, 3, 5 or 8 s, a target ("+") appeared and participants were instructed to respond to its onset with a button press as quickly as possible. **(B)** Mean reaction time across the ten-minute task in two-minute bins at baseline (teal) and follow-up (orange). Points and shading show the mean and 95% confidence interval. In a linear mixed-effects model, reaction time rose with time-on-task ($\beta = 7.9$ ms per bin, $p < 0.001$) and this did not differ between sessions (*session x bin* interaction $p = 0.45$). **(C)** Within-person change in mean reaction time (follow-up minus baseline). Clouds show the participant distribution and the point and whisker show the mean and its 95% confidence interval. Reaction time increased (mean = 10.5 ms, two-sided sign-flip permutation test, 10,000 permutations, Benjamini-Hochberg corrected across the three PVT measures, corrected $p = 0.020$). **(D)** Mean reaction time against age at both sessions with mixed-effects

JNeurosci Accepted Manuscript

lines. Line slope is the between-person age gradient and the offset between lines indicates the within-person change. **(E)** Mixed-effects coefficients for mean reaction time from the same model: within-person change (β = 10.53 ms), baseline age (β = -0.53 ms per year), and sex (β = -3.15 ms). The within-person change survived correction across the three PVT measures (corrected p = 0.017), whereas the age gradient did not (raw p = 0.034, corrected p = 0.102); sex did not differ from zero (p = 0.64, uncorrected). Error bars denote 95% confidence intervals, with significant terms in blue and non-significant in grey. n = 222 (training set) in B to E. *p < 0.05, ***p < 0.001.

Figure 3. Within-person aperiodic exponent decline tracks concurrent reaction time slowing in the PVT.

(A) Mean reaction time against the aperiodic exponent across pooled sessions at baseline (teal) and follow-up (orange). Lines and shading show the fit and 95% confidence interval from cluster-robust ordinary least-squares regression. Within-session Pearson correlations are annotated for reference and are uncorrected (baseline r = 0.10; follow-up r = -0.04). In the pooled model the exponent did not relate to reaction time (β = 15, uncorrected p = 0.46), though the slope was marginally more negative at follow-up (*exponent x session* β = -41.5 ms, uncorrected p = 0.049). **(B)** Within-person reaction time change against within-person exponent change. Participants with greater exponent decline slowed more (Pearson r(220) = -0.17, p = 0.010). **(C)** Reaction time change against the baseline exponent did not show a relationship (Pearson r(220) = 0.027, p = 0.69). **(D)** Coefficients from the full coupling model of reaction time change (ordinary least-squares with covariates: *exponent change, baseline age, their interaction, baseline exponent, baseline mean reaction time, sex, follow-up interval*). Each unit of exponent decline corresponded to a 91 ms increase in reaction time (*exponent change* β = -91.1 ms, Benjamini-Hochberg FDR-corrected p = 0.027 across the 108-test coupling grid, see

JNeurosci Accepted Manuscript

Methods). **(E)** Coefficients from the joint spectral model adding concurrent delta, theta, alpha and beta power changes. Only exponent change showed an association with reaction time slowing (β = -85.9 ms, FDR-corrected p = 0.006 across the five-term spectral family); the baseline spectral terms and demographic covariates are uncorrected. In A to C, points are individual participants. In A to E, bands and whiskers are 95% confidence intervals. In D and E, significant terms are in blue and non-significant in grey. n = 222 (training set) in A to E. † < 0.07, *p < 0.05, **p < 0.01, ***p < 0.001.

Figure 4. Response time in the modified Simon task slows and no-go accuracy improves within neurotypical adults.

(A) Schematic of the modified Simon Task. On each trial a single letter target ('H' or 'N') appeared to the left or right of a central fixation cross. On 'Go' trials, indicated by a surrounding circle, participants responded with the left hand to 'H' and with the right hand to 'N', irrespective of the side of stimulus presentation. 'Go' trials were congruent when the stimulus appeared on the same side as the responding hand and incongruent when it appeared on the opposite side; the Simon effect was defined as the mean response time difference between incongruent and congruent 'Go' trials. On 'No Go' trials, indicated by a surrounding diamond, participants were instructed to withhold their response. **(B-D)** Within-person change (follow-up minus baseline) in **(B)** overall 'Go' response time, **(C)** the Simon effect and **(D)** 'No Go' accuracy. Clouds show the participant distribution and the point and whisker show the mean and its 95% confidence interval. Response time increased (mean = 12.397 ms, two-sided sign-flip permutation test, 10,000 permutations, corrected p = 0.003) and 'No Go' accuracy improved (mean = 0.029, corrected $p < 1 \times 10^{-4}$), whereas the Simon effect did not change (mean = 1.163 ms, corrected p = 0.499). **(E-G)** Each measure against age at both sessions, baseline (teal) and follow-up (orange), with mixed-effects lines overlaid. In linear mixed-effects models, **(E)** older baseline

JNeurosci Accepted Manuscript

age was associated with slower response time (β = 2.227 ms per year, corrected p < 0.001), **(F)** a larger Simon effect (β = 0.448 ms per year, corrected p < 0.001) and **(G)** marginally lower no-go accuracy (β = -0.001 per year, corrected p = 0.053). Within participant effects are overlaid (in grey) as assessed in B-D. **(H-J)** Coefficients for each measure from a linear mixed-effects model (*within-person change, baseline age, sex*). All change and age terms survived correction within the three Simon measures except the Simon effect change (corrected p = 0.504) and the 'No Go' accuracy age gradient (corrected p = 0.053); sex did not differ from zero in any model (p = 0.34, 0.23 and 0.93, uncorrected). Error bars denote 95% confidence intervals, significant terms are in blue and non-significant in grey. n = 222 (training set) in B to J. † < 0.07, **p < 0.01, ***p < 0.001.

Figure 5. The aperiodic exponent does not track concurrent Simon measures.

(A) 'Go' response time against the aperiodic exponent across pooled sessions at baseline (teal) and follow-up (orange). Lines and shading show the fit and 95% confidence interval from cluster-robust ordinary least-squares regression. Within-session Pearson correlations are annotated for reference and are uncorrected (baseline r = -0.06; follow-up r = -0.17, p < 0.05). In the pooled model the exponent did not relate to response time (β = 16.67, uncorrected p = 0.48) and the slope did not change at follow-up (*exponent x session* β = -43 ms, uncorrected p = 0.11). **(B)** Within-person Go response-time change against exponent change did not show a relationship (Pearson r(220) = -0.02, p = 0.78). **(C)** Response-time change against the baseline exponent also did not show a relationship (Pearson r(220) = -0.03, p = 0.69). **(D)** Coefficients from the full coupling model of 'Go' response-time change (ordinary least-squares with covariates: *exponent change, baseline age, their interaction, baseline exponent, baseline reaction time, sex, follow-up interval*). Exponent change was not associated with slowing (β = -15.2 ms, Benjamini-Hochberg FDR-corrected p = 0.965 across the 108-test coupling grid),

JNeurosci Accepted Manuscript

though the model recovered age-related slowing (β = 1.3 ms per year, p < 0.001) and regression to the mean in baseline response time (β = -0.26, p < 0.001); covariate terms are uncorrected. **(E)** The same coupling model for Simon effect change showed no coupling with the exponent (β = -3.1, FDR-corrected p = 0.990 across the 108-test coupling grid), with baseline Simon effect being the only significant term (β = -0.479, p < 0.001, uncorrected). **(F)** The same coupling model for 'No Go' accuracy change also showed no coupling with the exponent (β = 0.084, FDR-corrected p = 0.965 across the 108-test coupling grid), with baseline 'No Go' accuracy the only significant term (β = -0.627, p < 0.001, uncorrected). Points in A to C are individual participants and the shaded band is the 95% confidence interval of the fit. In D to F, points are model coefficients and whiskers are 95% confidence intervals, with significant terms in blue and non-significant in grey. n = 222 (training set) in A to F. *p < 0.05, ***p < 0.001.

Figure 6. The aperiodic exponent and PVT slowing coupling is stable across training resamples, state-specific and domain-specific

Out-of-sample prediction of within-person PVT reaction time change across 200 age-stratified 80/20 resamples of the training set, fitted separately to pre-task (blue) and post-task (purple) EEG. Clouds show the distribution across resamples, and the point and whisker show the mean across resamples and its 95% confidence interval. **(A)** Ordinary least-squares coefficient relating exponent change to PVT reaction time change. The pre-task training-partition coefficient was negative in every resample (median = -93.46 ms) with 93% sign concordance between the independently fitted training and held-out partitions, whereas the post-task coefficient was near zero with an unstable sign (median = -2.08 ms, negative in 56.5% of resamples, 16% concordance). **(B)** Held-out R^2 of each model on the held-out partition of each resample (pre-task median R^2 = 0.167, RMSE = 51.1 ms, positive in 84% of resamples; post-task median R^2 = 0.122, RMSE = 52.0 ms, positive in 74%). Both arms are largely driven by baseline reaction

JNeurosci Accepted Manuscript

time (**Fig. 3D**). The paired difference in C isolates the pre-task contribution. **(C)** Paired difference in held-out R^2 (pre-task minus post-task) on the same participants (blue) beside a null obtained by permuting the outcome within each resample's training partition (grey). The mean paired increment exceeded a full label-shuffle null in a separate two-sided permutation test (observed mean $\Delta R^2 = 0.052$; null mean = -0.001, SD = 0.018; 1,000 global permutations x 100 folds, p = 0.008); asterisks denote that permutation test. Across the 200 resamples the increment had a median of 0.058 (mean 0.053) and a 2.5th-97.5th percentile spread of [-0.078, 0.162]. **(D)** Standardized elastic-net exponent weight (coefficient divided by the within-fold outcome standard deviation) for PVT reaction time pre-task (blue), PVT reaction time post-task (purple) and Simon 'Go' response time pre-task (grey). The pre-task PVT weight was consistently negative (median = -0.235), whereas the post-task PVT and pre-task Simon weights were negligible (median approximately 0). The weights were retained under the L1 penalty in 100%, 12% and 28% of resamples respectively; because the penalty was tuned within each arm, these rates are not directly comparable across arms. **(E)** The coupling coefficient refitted within the frozen 54-person held-out set (red diamond) against the distribution of held-out-partition coefficients from the training-set resamples (blue). The frozen coefficient was positive and non-significant ($\beta = 1.416$, p = 0.983), falling at the 93rd percentile of the resample distribution, and the out-of-sample R^2 of the frozen training model applied to the held-out set was negative (-0.181, worse than predicting the held-out mean), at the 2.5th percentile. Generalization is therefore supported by coefficient stability within the training sample rather than by the independent held-out test. n = 222 (training, resampled) for pre-task panels; n = 220 for post-task panels and for all paired pre-minus-post comparisons, two participants each lacking a post-task eyes-open recording at one session; n = 54 (frozen held-out set). **p < 0.01.

Table Legends

Neurosci Accepted Manuscript

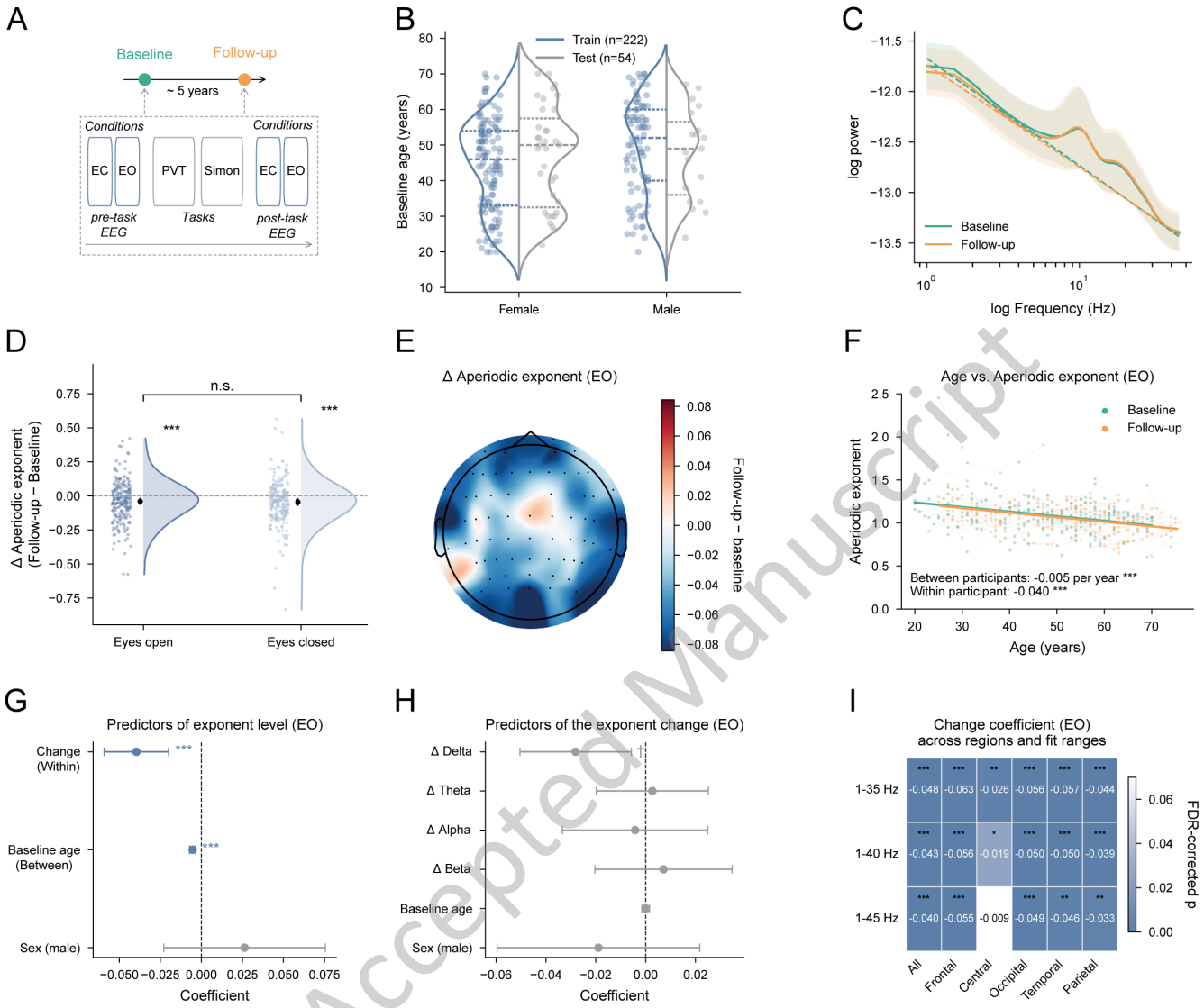
Table 1. Cohort characteristics for the training and held-out test splits.

Demographic and follow-up characteristics for the training split (n = 222), the *a priori* held-out test split (n = 54) and the full cohort (n = 276). N is the number of participants; Female is given as count (percentage); baseline age and the follow-up interval are given as mean (standard deviation, SD) with the observed range, where the follow-up interval is the per-participant elapsed time in years between the baseline and follow-up sessions.

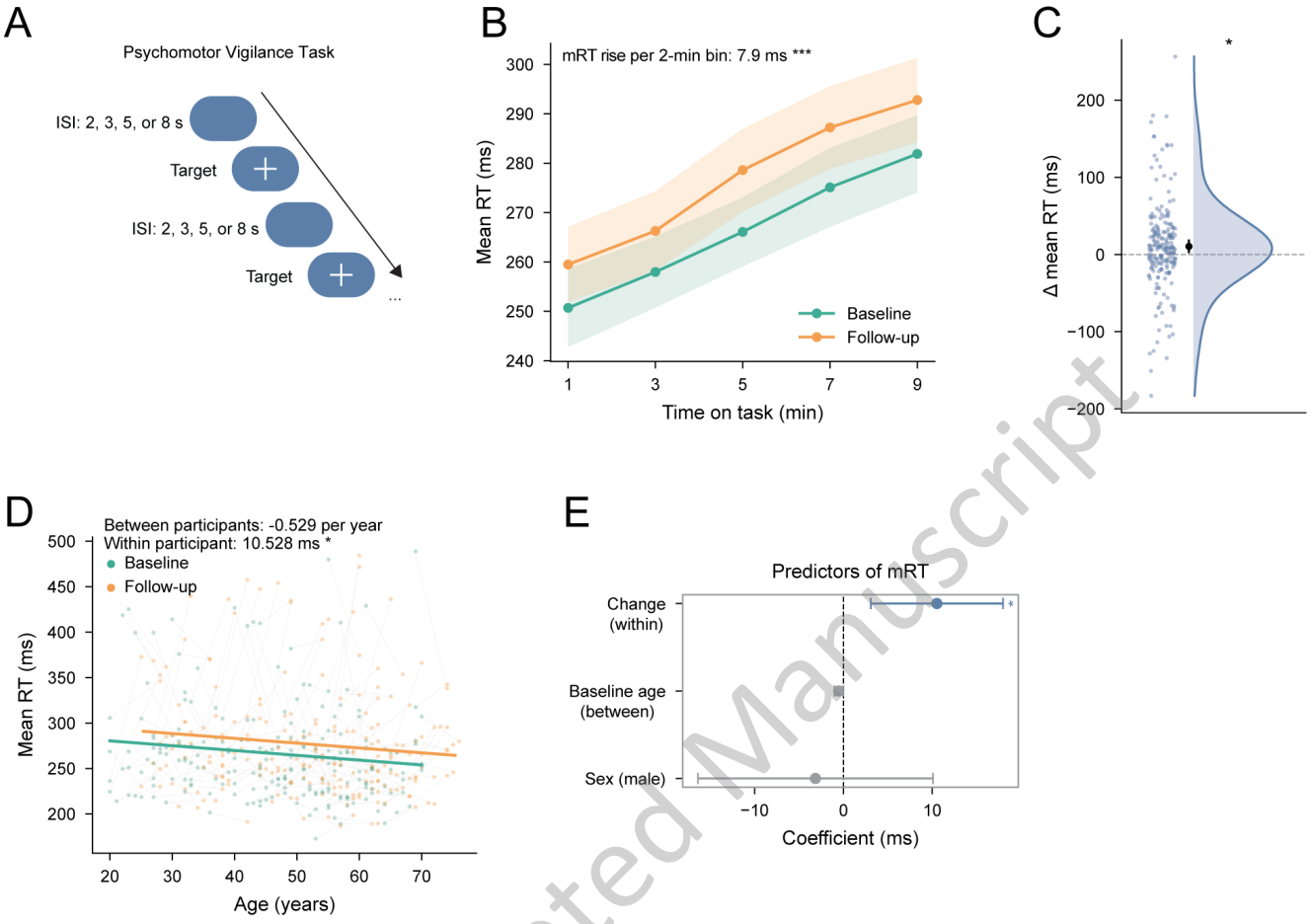
JNeurosci Accepted Manuscript

	Training Split	Held Out Test Split	Full cohort
N	222	54	276
Female, n (%)	131 (59.0%)	35 (64.8%)	166 (60.1%)
Baseline age, mean (SD)	46.581 (13.349)	47.185 (13.631)	46.699 (13.382)
Baseline age, range	20–70	22–70	20–70
Follow-up interval (yr), mean (SD)	5.365 (0.771)	5.111 (0.744)	5.315 (0.771)
Follow-up interval (yr), range	4–8	4–7	4–8

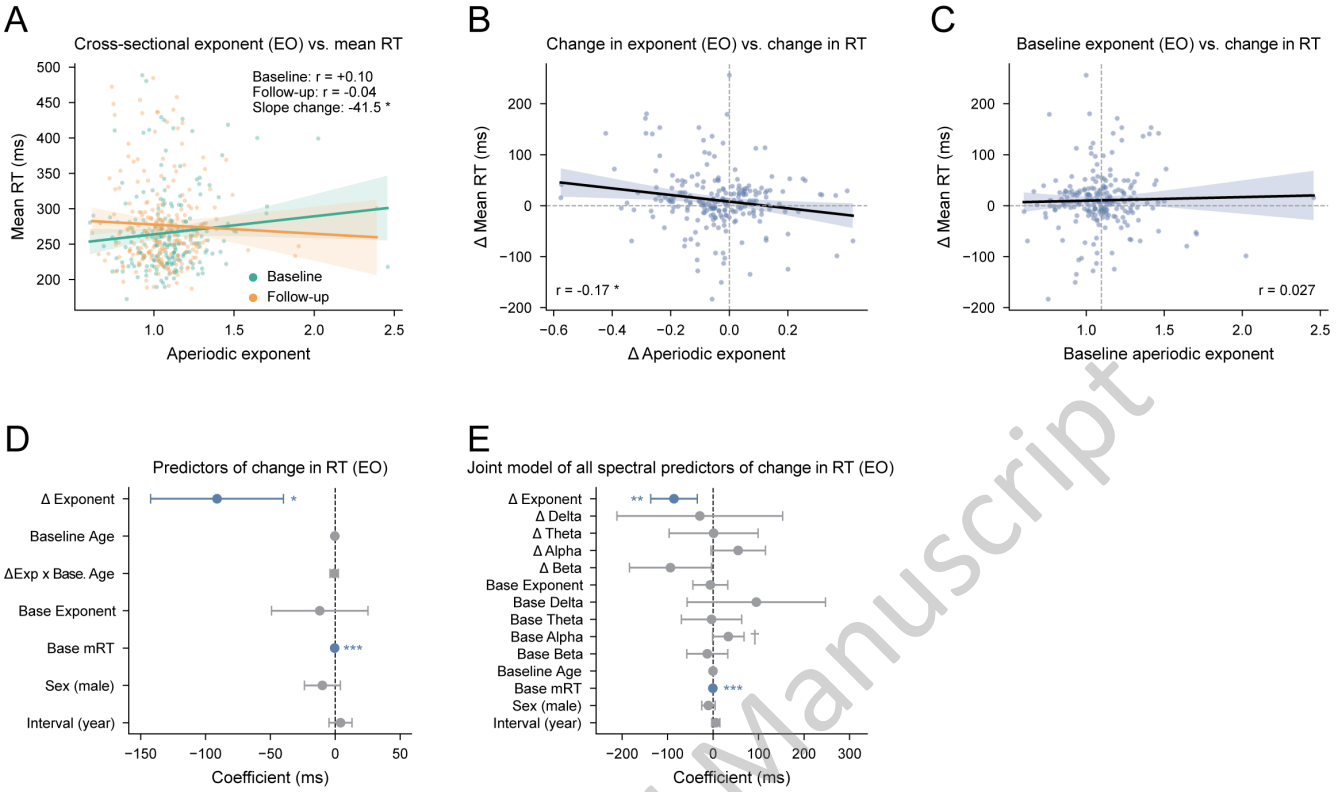
JNeurosci Accepted Manuscript



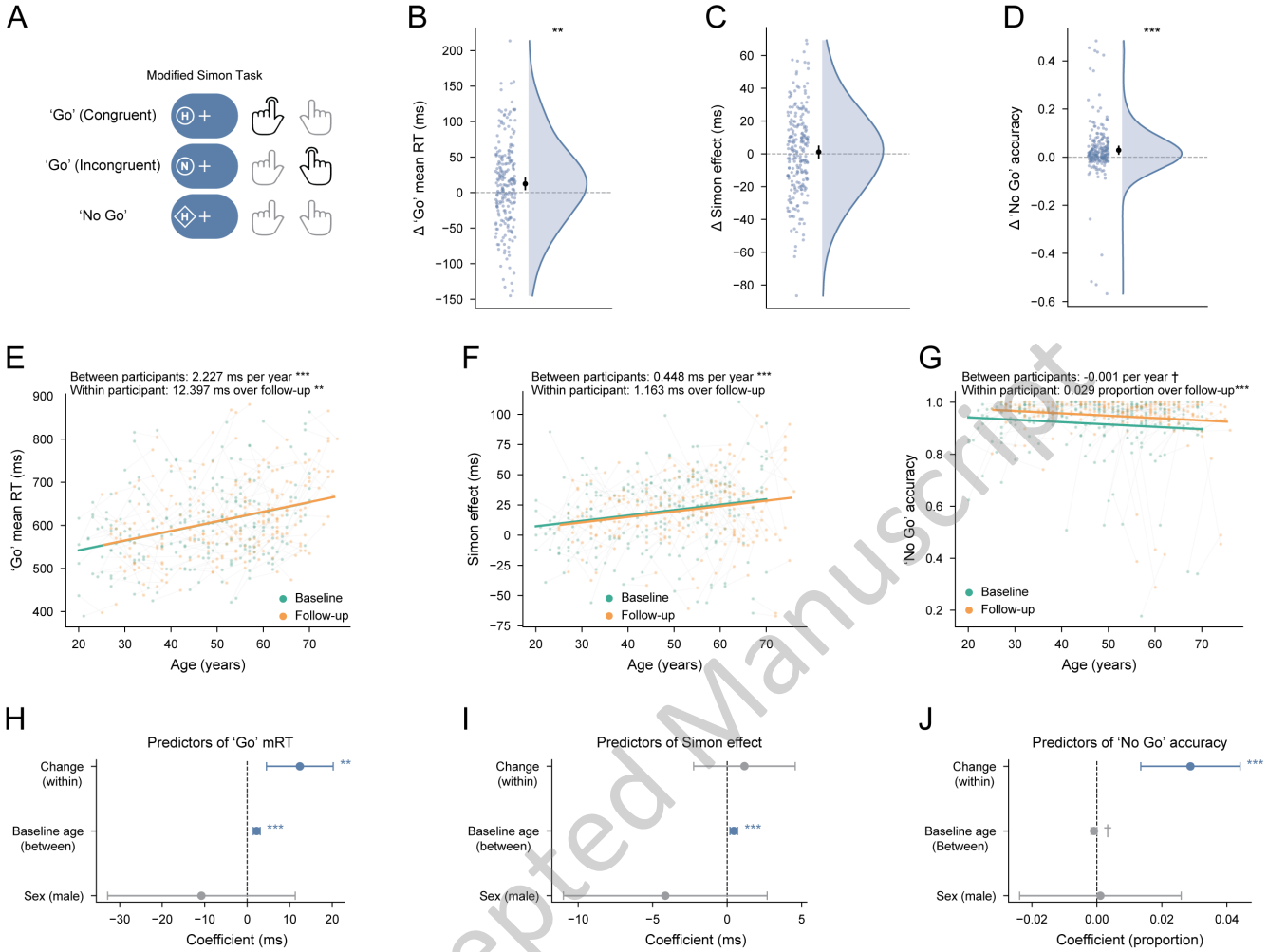
JNeurosci Accepted Manuscript



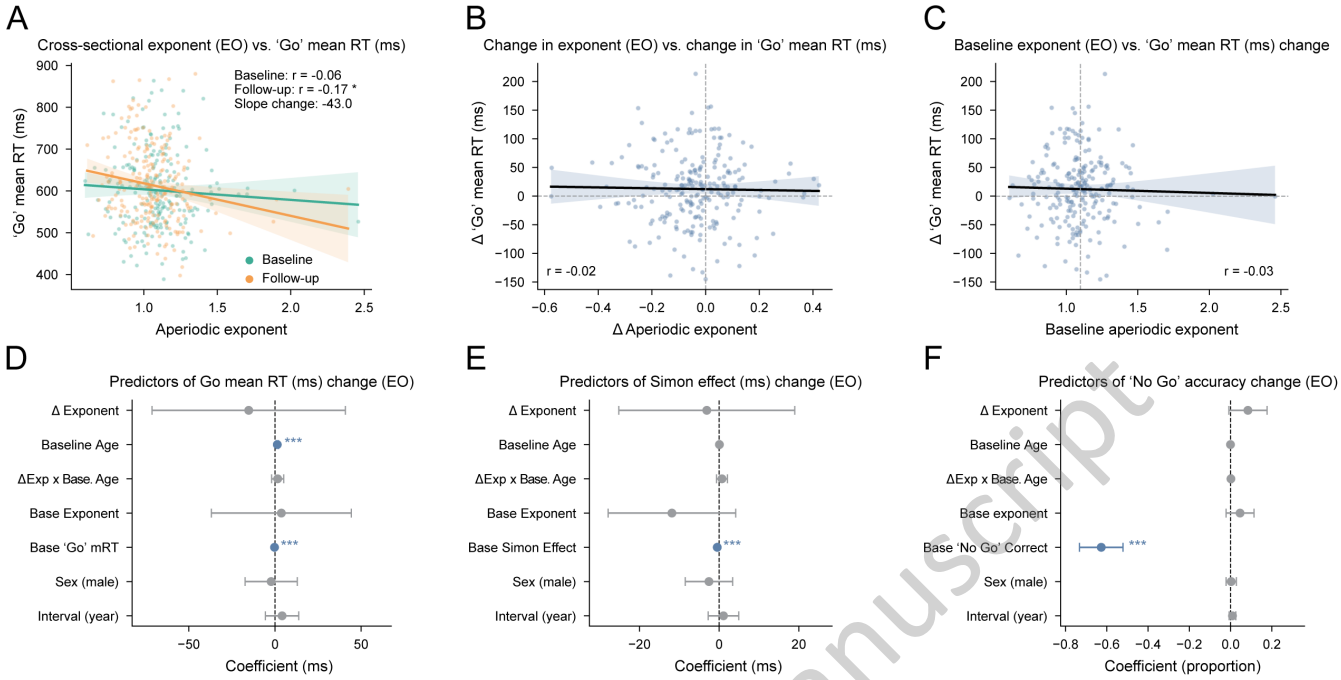
JNeurosci Accepted Manuscript



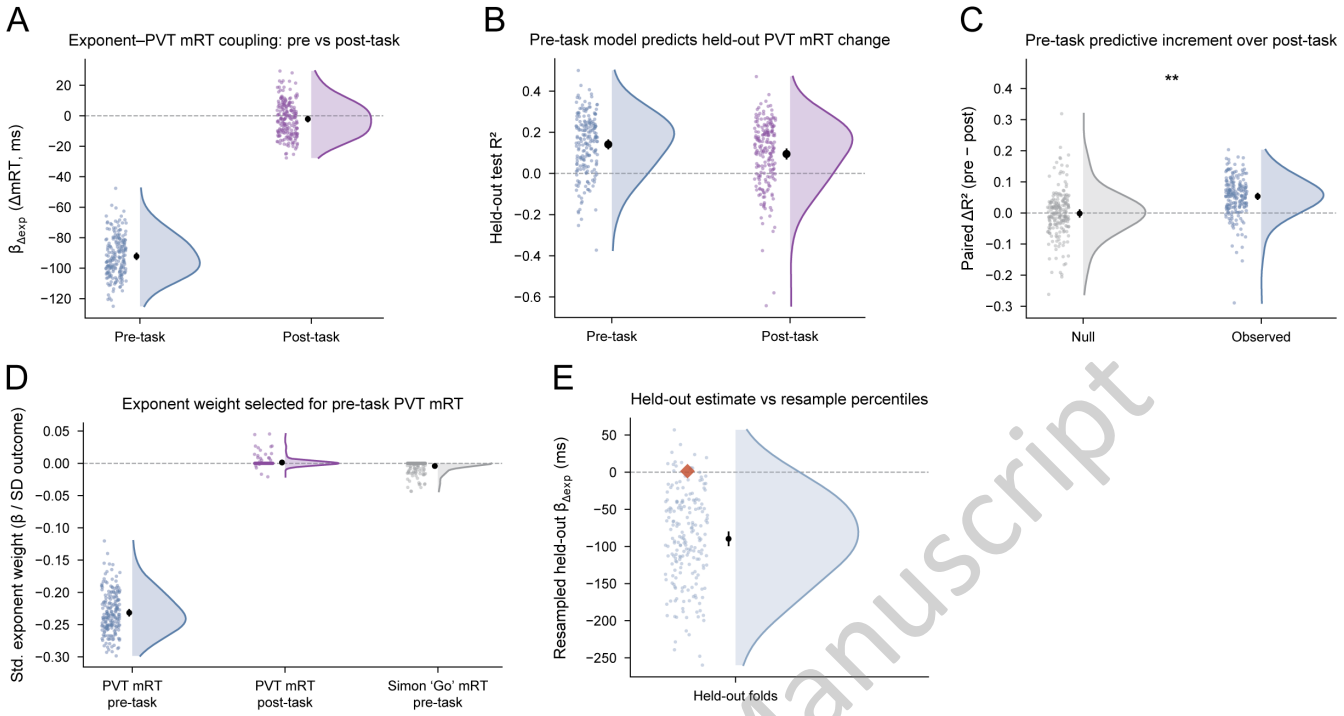
JNeurosci Accepted Manuscript



JNeurosci Accepted Manuscript



JNeurosci Accepted Manuscript



JNeurosci Accepted Manuscript